NATIONAL ADVISORY COMMITTEE FOR AERONAUTICS

TECHNICAL NOTE

No. 1547

TANK TESTS OF THREE TYPES OF AFTERBODIES ON A FLYING-BOAT MODEL WITH BASIC HULL LENGTH-BEAM RATIO OF 10.0

By Charlie C. Garrison and Eugene P. Clement

Langley Memorial Aeronautical Laboratory
Langley Field, Va.

Washington
March 1948

NATIONAL ADVISORY COMMITTEE FOR AERONAUTICS

TECHNICAL NOTE NO. 1547

TANK TESTS OF THREE TYPES OF AFTERBODIES ON A FLYING-BOAT MODEL WITH BASIC HULL LENGTH-BEAM RATIO OF 10.0

By Charlie C. Garrison and Eugene P. Clement

SUMMARY

Three different types of afterbodies were tested on a powered dynamic model of a flying boat having a basic length-beam ratio of 10.0. An afterbody with constant dead rise, an afterbody with warped dead rise, and an afterbody of extended length with warped dead rise were tested. The minimum depth of step for adequate landing stability was determined for each afterbody. The required depth of step at the centroid was 15.0 percent of the beam for the constant-dead-rise afterbody, 13.0 percent of the beam for the warped-dead-rise afterbody, and 21.8 percent of the beam for the extended warped-dead-rise afterbody.

Take-off stability and spray characteristics were determined for each afterbody with the minimum depth of step for adequate landing stability. The upper and lower trim limits of stability were determined for the constant-dead-rise afterbody and the warped-dead-rise afterbody, and were found to be almost the same. It was found that satisfactory take-offs (2° maximum amplitude of porpoising) could be made over a range of position of the center of gravity of 15 percent mean aerodynamic chord for the constant-dead-rise afterbody, 9 percent mean aerodynamic chord for the warped-dead-rise afterbody, and 15 percent mean aerodynamic chord for the extended warped-dead-rise afterbody. The spray characteristics for each afterbody were satisfactory.

INTRODUCTION

Wind-tunnel and towing-tank tests of the past few years have shown that, for flying boats, the use of hulls of high length-beam ratio allows the air drag to be reduced (reference 1) while the hydrodynamic performance is maintained (references 2 and 3). Extensive data have not been made available, however, upon which to base the design of the afterbody of a hull of high length-beam ratio. In order to provide information for design, three different types of afterbodies were tested in smooth water on a powered dynamic model having a basic length-beam ratio of 10.0.

The model was a $\frac{1}{10}$-size model of a hypothetical, large flying boat having a relatively high wing loading and a low power loading. An afterbody with constant dead rise, an afterbody of the same length with warped dead rise, and an afterbody of extended length with warped dead rise were included in the investigation.

The three afterbodies were tested for landing stability, take-off stability, and spray characteristics. The first part of the tests was to determine by means of landing tests the minimum acceptable depth of step for each afterbody. Since the air drag and, therefore, the depth of step for the conventional seaplane should be kept to a minimum, the choice of afterbody type depends, in part, on the depth of step required with each type. The three afterbodies were further evaluated by making take-off and spray tests with the mimimum depth of step for adequate landing stability.

SYMBOLS

C_{Δ_o} gross load coefficient $\left(\frac{\Delta_o}{wb^3}\right)$

C_L aerodynamic lift coefficient $\left(\frac{\text{Lift}}{\frac{1}{2}\rho S V^2}\right)$

C_m aerodynamic pitching-moment coefficient $\left(\frac{\text{Pitching-moment}}{\frac{1}{2}\rho S V^2 \bar{c}}\right)$

T_e effective thrust, pounds $\left(T_e = T - \Delta D = D + R\right)$

k forebody spray coefficient $\left(\frac{C_{\Delta_o}}{\left(\frac{L_f}{b}\right)^2}\right)$

τ_L landing trim (angle between base line of hull and water plane at initial contact), degrees

b maximum beam over chines, feet

$\bar{c}$ mean aerodynamic chord (M.A.C.), feet

D drag of model without propellers, pounds

ΔD increase in drag due to slipstream, pounds

Δ_o	gross load, pounds
L_f	length of forebody from bow to step centroid, feet
R	measured resultant horizontal force with power on, pounds
ρ	density of air, slugs per cubic foot
S	area of wing, square feet
T	propeller thrust, pounds
V	carriage speed (approx. 95 percent of airspeed), feet per second
w	specific weight of water (63.3 lb/cu ft for these tests)

DESCRIPTION OF MODEL

The model, designated Langley tank model 228, was a $\frac{1}{10}$-size, powered, dynamic model of a hypothetical flying boat having a gross weight of 125,000 pounds, a wing loading of 59.5 pounds per square foot, and a power loading of 9.47 pounds per horsepower. The basic length-beam ratio of the hull was 10.0, and the gross load coefficient C_{Δ_o} was 1.95.

The general arrangement of the model with the constant-dead-rise afterbody is shown in figure 1. The aerodynamic and propulsive characteristics of the model and the dimensions of the forebody and the three afterbodies are given in table I.

The dead rise of the forebody was $22\frac{1}{2}^\circ$ for approximately $\frac{3}{4}$ beam forward of the step and increased forward of this point to form a sharp bow. The length of the forebody was 5.88 beams. The constant-dead-rise afterbody and the warped-dead-rise afterbody were 4.12 beams in length, and the extended warped-dead-rise afterbody was 6.63 beams in length. The afterbodies are shown in figure 2. With the constant-dead-rise afterbody the model was designated model 228D, with the warped-dead-rise afterbody, model 228E, and with the extended warped-dead-rise afterbody, model 228F. The length-beam ratio of models 228D and 228E was 10.0, and the length-beam ratio of model 228F was 12.5. The depth of step was changed by raising or lowering the afterbodies. The depths of step tested with each afterbody and the corresponding model designations are given in table II. In the model designation, the numerical value following the dash is the depth of the step at the centroid in percent of the beam. The model was also tested without an afterbody and was designated model 228Z.

The power plant consisted of four 2-horsepower, three-phase, variable-frequency, alternating-current induction motors. Each motor turned a four-blade, dural propeller of the paddle-wheel square-tip type. The elevators were controlled from the towing carriage. Slats were attached to the leading edge of the wing in order to make the angle of stall and the maximum lift coefficient correspond to full-size values.

The pitching moments of inertia of the ballasted model were as follows:

Pivot position (percent M.A.C.)	Moment of inertia (slugs per sq ft)
20	16.8
37	13.5

APPARATUS AND PROCEDURE

The tests were made in Langley tank no. 1 which is described in reference 4. The methods of testing dynamic models are described in reference 5. The model was tested at the 6-foot water level under the center of the towing carriage where the air flow is parallel to the water surface and the airspeed is approximately 5 percent higher than the carriage speed. The carriage speed is used in the presentation of aerodynamic and hydrodynamic data in the present paper. The model was free to trim about the pivot, which was located at its ballasted center-of-gravity position, and was free to move vertically but was restrained in roll and yaw.

During the landing and take-off tests, continuous records of the rise of the pivot and trim were made by means of electrical slide-wire bridges connected to a recording oscillograph. The speed of the carriage was recorded, and electrical contacts located flush with the keel of the model at the step and the sternpost registered deflections on the record when these points entered and left the water.

RESULTS

Aerodynamic characteristics.- The variation of the effective take-off thrust of the model with speed together with the estimated scale

thrust of the full-size flying boat, is shown in figure 3. The effective thrust of the model was equal to the scale thrust of the full-size seaplane at approximately one-half of the get-away speed. The effective thrust of the model was obtained from the following expression:

$$T_e = T - \Delta D$$

$$T - \Delta D = D + R$$

The values of D and R were determined by towing the model at 0° trim with the step 8 inches above the surface of the water and with elevators and flaps set at 0°.

Values of the lift and pitching moments were determined at various speeds and trims with the model in the air in the same position as for the determination of the thrust. The moments were taken about a point corresponding to a center-of-gravity location of 25 percent of the mean aerodynamic chord. Data were obtained with zero thrust, flaps deflected 50°, elevators deflected -15°, and a speed of 40 feet per second. The results are plotted in coefficient form in figure 4. Data were also obtained with take-off thrust, flaps deflected 20°, and elevators set at 0°. The results are given in figure 5 as a plot of lift and pitching moment against speed.

Hydrodynamic characteristics.- Landings were made with each afterbody at several depths of step over the entire range of practicable landing trim (approx. 4° to 12°). The flaps were deflected 50°, and the deceleration was approximately 2 feet per second per second. Static effective thrust for the landings was 11.6 pounds (one-fourth the static effective thrust for take-off). Landings of models 228D-12.0 and 228D-15.0 were made with the center of gravity located at 26 percent and 34 percent mean aerodynamic chord; the landings of the other models were made with the center of gravity located at 34 percent mean aerodynamic chord. The landing tests to determine the minimum depth of step for each afterbody were made with the center of gravity at 34 percent mean aerodynamic chord because the tests of models 228D-12.0 and 228D-15.0 showed that the landings at 34 percent mean aerodynamic chord were less stable than those at 26 percent mean aerodynamic chord.

Figure 6 is a photograph of a typical oscillograph record taken during a landing of model 228D-17.0. This record shows one skip (that is, the step left the water one time). Sinking speed and angular velocity at contact were obtained from the records by determining the slopes of

the rise and trim traces with respect to time. The sinking speeds at contact varied from approximately 0.4 to 1.2 feet per second. The trim of the model was generally decreasing at contact because of the change in aerodynamic pitching moments as the model approached the water. The rate of decrease in trim at contact averaged about 1.5° per second.

Time histories showing the variation of rise, trim, and carriage speed for four landings each of models 228D-12.0, 228E-10.8, and 228F-18.4 are presented in figure 7. Each of these three models had an insufficient depth of step for satisfactory landing stability, and the landing histories show the character of the landing instability for the different afterbodies. The points shown in figures 7(b) and 7(c) at which the step entered and left the water were determined from the contact deflection on the records. Points at which the sternpost first entered the water are shown only for the landings at high trim for which the sternpost entered before the step.

The number of skips and the maximum and minimum trim and rise during the greatest skipping cycles of each landing were determined. These data are presented for model 228D-12.0, with the center of gravity located at 34 percent and 26 percent mean aerodynamic chord, in figure 8. The results for models 228E-10.8 and 228F-18.4, with the center of gravity at 34 percent mean aerodynamic chord, are presented in figures 9 and 10. Similar plots were prepared for the other models, and envelope curves were faired through the points of maximum and minimum trim and rise and the maximum number of skips. The envelope curves for each afterbody with three depths of step are presented in figure 11. The envelope curves for the landings of the model with no afterbody, model 228Z, are also presented for comparison in figure 11.

The maximum number of skips, the maximum change in trim, and the maximum change in rise encountered with each afterbody for each depth of step were determined from the envelope curves and are presented in figure 12.

Trim limits of stability determined at constant speeds for model 228D-15.0 and 228E-14.9 with take-off thrust and flaps deflected 20° are presented in figure 13.

Tests to determine the variation of trim with speed during take-off were made with take-off thrust, flaps deflected 20°, and an acceleration of approximately 1 foot per second per second for models 228D-15.0, 228E-14.9, and 228F-21.8. The elevators were set at 0° and -15°. Representative trim tracks for various positions of the center of gravity are shown in figure 14. Results are presented in figure 15 for the variation of maximum amplitude of porpoising with position of the center of gravity. A comparison of the maximum porpoising amplitudes for the three afterbodies is shown in figure 16. The effect of elevator deflection on the range of position of the center of gravity for satisfactory take-off

(2° maximum amplitude of porpoising) is shown in figure 17.

The range of speed in which spray struck the propellers and flaps of model 228D-15.0 during take-off was determined. The results are presented in figure 18. The tests were made with take-off thrust, flaps deflected 20°, elevators at 0°, and the center of gravity located at 30 percent mean aerodynamic chord. Gross loads of 113.5, 123.5, 136.0, and 145.0 pounds were investigated.

DISCUSSION

Each of the afterbodies was tested with depths of step insufficient for satisfactory landing stability and with depths of step adequate or more than adequate for satisfactory landing stability. The character of the landings when the depths of step were insufficient for satisfactory landing stability is shown in the time histories of figure 7. In each of these landings the trim of the model increased just after the step entered the water; aerodynamic and hydrodynamic lift were then increased because of the increased angle of attack of the wing and forebody bottom, and the model left the water. This cycle was repeated during each skip. As the speed of the towing carriage decreased, the tendency of the model to skip decreased and the model became stable. When landings were made with the afterbody removed, the model increased in trim after contact and usually left the water once. Part of the skipping tendency, therefore, was independent of afterbody form or depth of step and is attributed to the character of the forebody lines. The skipping of the complete model was more severe than that of the model with the afterbody removed. The contribution of the afterbody to the skipping tendency is explained in reference 6. The skipping is caused by the flow from the forebody bottom creating a suction on the bottom of the afterbody at high speeds. The suction force causes the model to increase in trim and to skip out of the water. During landings at high trims the skipping of the model with either of the warped afterbodies was further aggravated by upper-limit porpoising. A large number of landings was required to determine the maximum skipping instability of each model for the entire range of practicable landing trim because of the effect of such variables as sinking speed and angular velocity at contact.

The important relationship of depth of step to landing stability can be seen from the envelope curves of figure 11. There is a large improvement in the landing characteristics for each afterbody with increase in depth of step. Landing trim is also an important variable. There are pronounced peaks in the plots of rise at greatest cycle

against landing trim in figure 11. The largest changes in rise occurred for landings at about 5° trim for the constant-dead-rise afterbody, for landings at about 7° trim for the warped-dead-rise afterbody, and for landings at about 9° trim for the extended warped-dead-rise afterbody.

The maximum number of skips and the maximum changes in trim and rise for the range of practicable landing trim are all quantities which define in part the skipping instability of a particular model. Maximum change in rise is probably the most important of the three. It can be seen in figure 12 that as the depths of step for the two basic afterbodies were increased from the minimum depths tested, the maximum change in rise at first decreased rapidly. As the rise amplitudes approached the value for the model with no afterbody, however, the decrease in rise amplitude with increase in depth of step was almost negligible. For the range of depth of step tested on the extended afterbody, the rate of decrease in rise amplitude with increase in depth of step was small and relatively uniform. The maximum number of skips and the maximum change in trim for each of the afterbodies, in general, varied with depth of step in the same manner as the maximum change in rise. The maximum skipping amplitudes for model 228D-12.0 were much less severe with the center of gravity at 26 percent mean aerodynamic chord than with the center of gravity at 34 percent mean aerodynamic chord.

On the basis of figure 12 the minimum acceptable depth of step for satisfactory landing stability for each of the three afterbodies was decided to be as follows:

Afterbody	Depth of step at centroid (percent beam)	Step area (sq in.)
Constant-dead-rise	15.0	22.8
Warped-dead-rise	13.0	19.0
Extended warped-dead-rise	21.8	31.8

Depths of step that had been tested were selected for each afterbody. The first depths of step on the safe side of the breaks in the rise curves of figure 12 were selected for models 228D and 228E. The depth of step that gave approximately the same maximum change in rise as for these two afterbodies was selected for the extended afterbody. For

comparable landing stability the step area required for the warped-dead-rise afterbody was approximately 3.8 square inches less than that required for the constant-dead-rise afterbody and approximately 12.8 square inches less than that required for the extended warped-dead-rise afterbody. The air drag of the step for the warped-dead-rise afterbody would therefore be expected to be less than the air drag of the steps for the other two afterbodies.

Tests were made to determine the take-off stability of each afterbody with the minimum depth of step for adequate landing stability. Take-off tests were made with models 228D-15.0, 228E-14.9, and 228F-21.8. Model 228E-14.9 had a depth of step slightly greater than the minimum for adequate landing stability but the effect of this difference on take-off stability is considered to be insignificant. The trim limits of stability for models 228D-15.0 and 228E-14.9 (fig. 13) are almost the same and indicate that in this case warping the afterbody has no appreciable effect on the trim limits. Figure 14, however, shows that model 228E-14.9 encountered upper-limit porpoising with elevators deflected -15° at positions of the center of gravity for which model 228D-15.0 was stable. At positions of the center of gravity of 28 percent, 30 percent, and 32 percent mean aerodynamic chord, model 228E-14.9 trimmed up abruptly at about 38 feet per second and began porpoising. For the same positions of the center of gravity, model 228D-15.0 trimmed up more slowly and a smaller amount than model 228E-14.9 and remained stable.

Figure 17 shows that satisfactory take-offs could be made with a fixed elevator deflection of -15° at positions of the center of gravity from 20.0 to 35.0 percent mean aerodynamic chord for model 228D-15.0, 20.4 to 29.3 percent mean aerodynamic chord for model 228E-14.9, and approximately 18.3 to 33.3 percent mean aerodynamic chord for model 228F-21.8. The range of position of the center of gravity for satisfactory take-offs for models 228D-15.0 and 228F-21.8 was 15 percent mean aerodynamic chord whereas the range for model 228E-14.9 was only 9 percent mean aerodynamic chord.

The observations made and the spray data obtained indicated that the spray characteristics of models 228D-15.0, 228E-13.0, and 228F-21.8 were satisfactory as was to be expected since the value of the spray criterion k (reference 3) is 0.065, which is in the region for light spray. Spray in the propellers and flaps during take-offs and landings at the design gross load was not excessive for any of the three models. During take-offs of the models, the forebody blister wetted the horizontal tail at speeds above 20 feet per second. This spray, which was broken up by the action of the slipstream, was not heavy. During the landing runouts (one-fourth take-off thrust), the slipstream did not

break up this blister and, consequently, a heavy jet of water struck the tail. At high speeds, intermittent spray on the horizontal tail caused a small oscillation in trim (less than 2°) during take-offs. The speeds at which this oscillation occurred are indicated by short vertical lines on the trim tracks of figure 14.

CONCLUSIONS

Three types of afterbodies were tested on a $\frac{1}{10}$-size powered dynamic model of a large flying boat having a basic length-beam ratio of 10.0. Landing, take-off, and spray tests were made with a constant-dead-rise afterbody, a warped-dead-rise afterbody, and an extended warped-dead-rise afterbody. The results of the tests indicated the following conclusions:

1. The minimum depth of step at the centroid for satisfactory landing stability was 15.0 percent of the beam for the constant-dead-rise afterbody, 13.0 percent of the beam for the warped-dead-rise afterbody, and 21.8-percent of the beam for the extended warped-dead-rise afterbody.

2. With the minimum depth of step for adequate landing stability, the upper and lower trim limits of stability for the constant-dead-rise afterbody and the warped-dead-rise afterbody were almost the same.

3. With the minimum depth of step for adequate landing stability, satisfactory take-offs (2° maximum amplitude of porpoising) could be made with a fixed elevator deflection of -15° over a range of center-of-gravity positions of 15 percent mean aerodynamic chord for the constant-dead-rise afterbody, 9 percent mean aerodynamic chord for the warped-dead-rise afterbody, and 15 percent mean aerodynamic chord for the extended warped-dead-rise afterbody.

4. The spray characteristics for each afterbody with the minimum depth of step for adequate landing stability were satisfactory.

Langley Memorial Aeronautical Laboratory
National Advisory Committee for Aeronautics
Langley Field, Va., November 24, 1947

REFERENCES

1. Yates, Campbell C., and Riebe, John M.: Effect of Length-Beam Ratio on the Aerodynamic Characteristics of Flying-Boat Hulls. NACA TN No. 1305, 1947.

2. Benson, James M., and Bidwell, Jerold M.: Bibliography and Review of Information Relating to the Hydrodynamics of Seaplanes. NACA ACR No. L5G28, 1945.

3. Parkinson, John B.: Design Criterions for the Dimensions of the Forebody of a Long-Range Flying Boat. NACA ARR No. 3K08, 1943.

4. Truscott, Starr: The Enlarged N.A.C.A. Tank, and Some of Its Work. NACA TM No. 918, 1939.

5. Truscott, Starr, and Olson, Roland E.: The Longitudinal Stability of Flying Boats as Determined by Tests of Models in the NACA Tank. II - Effect of Variation in Form of Hull on Longitudinal Stability. NACA ARR, Nov. 1942.

6. Parkinson, John B.: Notes on the Skipping of Seaplanes. NACA RB No. 3I27, 1943.

TABLE I

AERODYNAMIC AND PROPULSIVE CHARACTERISTICS AND HULL DIMENSIONS OF LANGLEY TANK MODEL 228 AND FULL-SIZE FLYING BOAT

	$\frac{1}{10}$-size model	Full-size flying boat
Design gross load, lb	123.5	125,000
Gross load coefficient, C_{Δ_o}	1.95	1.95
Wing area, sq ft	21.0	2,100
Take-off horsepower	4.17	13,200
Wing loading, lb/sq ft	5.88	59.5
Power loading, lb/hp	29.6	9.47
Over-all length, in.	151.7	1517.0
Location of centroid of step, percent M.A.C.	36.1	36.1
Height of center of gravity above base line, in.	17.22	172.2
Wing:		
Span, in.	174	1,740
Angle of wing setting to base line, deg	5.0	5.0
Mean aerodynamic chord (M.A.C.), in.	18.9	189
Leading edge, M.A.C.		
Aft of bow, in.	63.7	637
Above base line, in.	22.2	222
Flaps (slotted)		
Take-off deflection, deg	20	20
Landing deflection, deg	50	50
Horizontal tail surfaces:		
Span, in.	66.4	664
Leading edge at root		
Aft of bow, in.	130.36	1303.6
Above base line, in.	24.83	248.3
Angle of stabilizer to base line, deg	-1.0	-1.0
Dihedral, deg	10.0	10.0
Propellers:		
Number	4	4
Blades	4	4
Diameter, in.	18.1	181
Blade angle (3/4 radius), deg	10.0	—
Revolutions per minute with full power	5250	—
Angle of thrust line to base line, deg	2.0	2.0

TABLE I — Concluded

AERODYNAMIC AND PROPULSIVE CHARACTERISTICS AND HULL DIMENSIONS

OF LANGLEY TANK MODEL 228 AND FULL-SIZE FLYING BOAT — Concluded

	$\frac{1}{10}$-size model	Full-size flying boat
Forebody of hull:		
Maximum beam, in.	12.0	120
Length from bow to centroid of step, in.	70.49	704.9
Angle of step (V-type), deg	30	30
Angle of forebody keel to base line, deg	0	0
Angle of dead rise at step, deg		
Excluding chine flare	22.5	22.5
Including chine flare	18.0	18.0
Extent of constant dead rise from centroid of step, beams	3/4	3/4
Constant-dead-rise afterbody:		
Length from centroid of step to sternpost, in.	49.51	495.1
Length-beam ratio	4.13	4.13
Angle of afterbody keel, deg	6.5	6.5
Angle of dead rise, deg	22.5	22.5
Warped-dead-rise afterbody:		
Length from centroid of step to sternpost, in.	49.51	495.1
Length-beam ratio	4.13	4.13
Angle of afterbody keel, deg	6.5	6.5
Extended warped-dead-rise afterbody:		
Length from centroid of step to sternpost, in.	79.61	796.1
Length-beam ratio	6.63	6.63
Angle of afterbody keel, deg	8.5	8.5

TABLE II

MODEL DESIGNATIONS AND STEP DATA

Afterbody	Langley tank model	Depth of Step						Step area (sq in)	Sternpost angle (deg)
		At keel		At centroid		Mean			
		Inches	Percent beam	Inches	Percent beam	Inches	Percent beam		
Constant-dead-rise	228D-12.0	1.69	14.1	1.44	12.0	1.54	12.8	18.5	8.5
	228D-13.6	1.88	15.7	1.63	13.6	1.73	14.3	20.7	8.7
	228D-15.0	2.05	17.1	1.80	15.0	1.90	15.8	22.8	8.9
	228D-17.0	2.29	19.1	2.04	17.0	2.14	17.8	25.7	9.2
Warped-dead-rise	228E-8.9	.97	8.1	1.07	8.9	1.09	9.1	13.1	7.7
	228E-10.8	1.19	9.9	1.29	10.8	1.31	10.9	15.7	7.9
	228E-11.7	1.31	10.9	1.41	11.7	1.43	11.9	17.2	8.1
	228E-13.0	1.46	12.2	1.56	13.0	1.58	13.2	19.0	8.3
	228E-14.9	1.69	14.1	1.79	14.9	1.81	15.1	21.7	8.5
	228E-17.9	2.05	17.1	2.15	17.9	2.17	18.1	26.0	8.9
	228E-19.9	2.29	19.1	2.39	19.9	2.41	20.1	28.9	9.2
Extended warped-dead-rise	228F-11.7	1.31	10.9	1.40	11.7	1.43	11.9	17.2	9.4
	228F-18.4	2.12	17.7	2.21	18.4	2.24	18.7	26.9	9.9
	228F-21.8	2.53	21.1	2.62	21.8	2.65	22.1	31.8	10.2

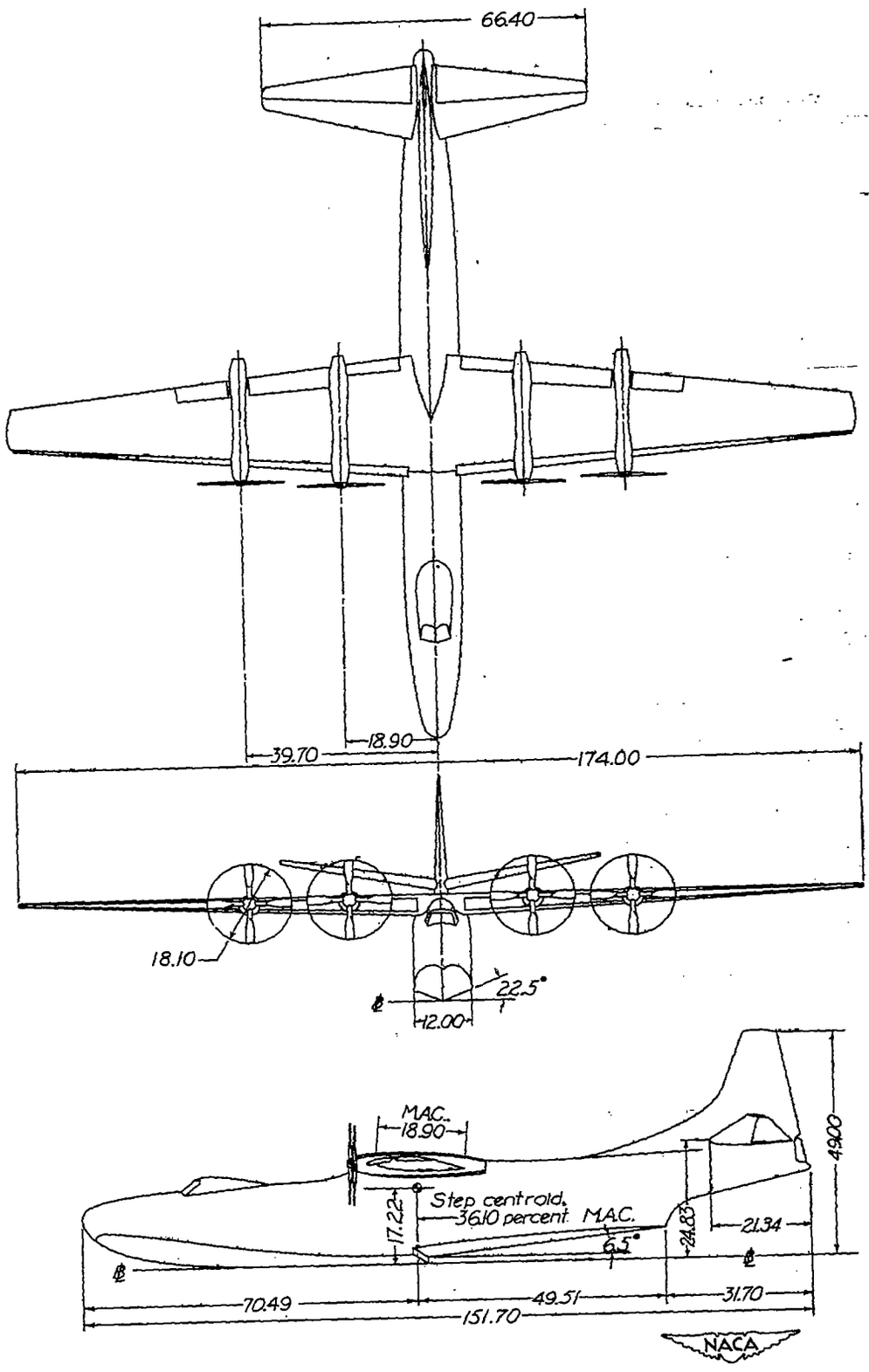

Figure 1.- General arrangement of Langley tank model 228D.
(Dimensions are in inches.)

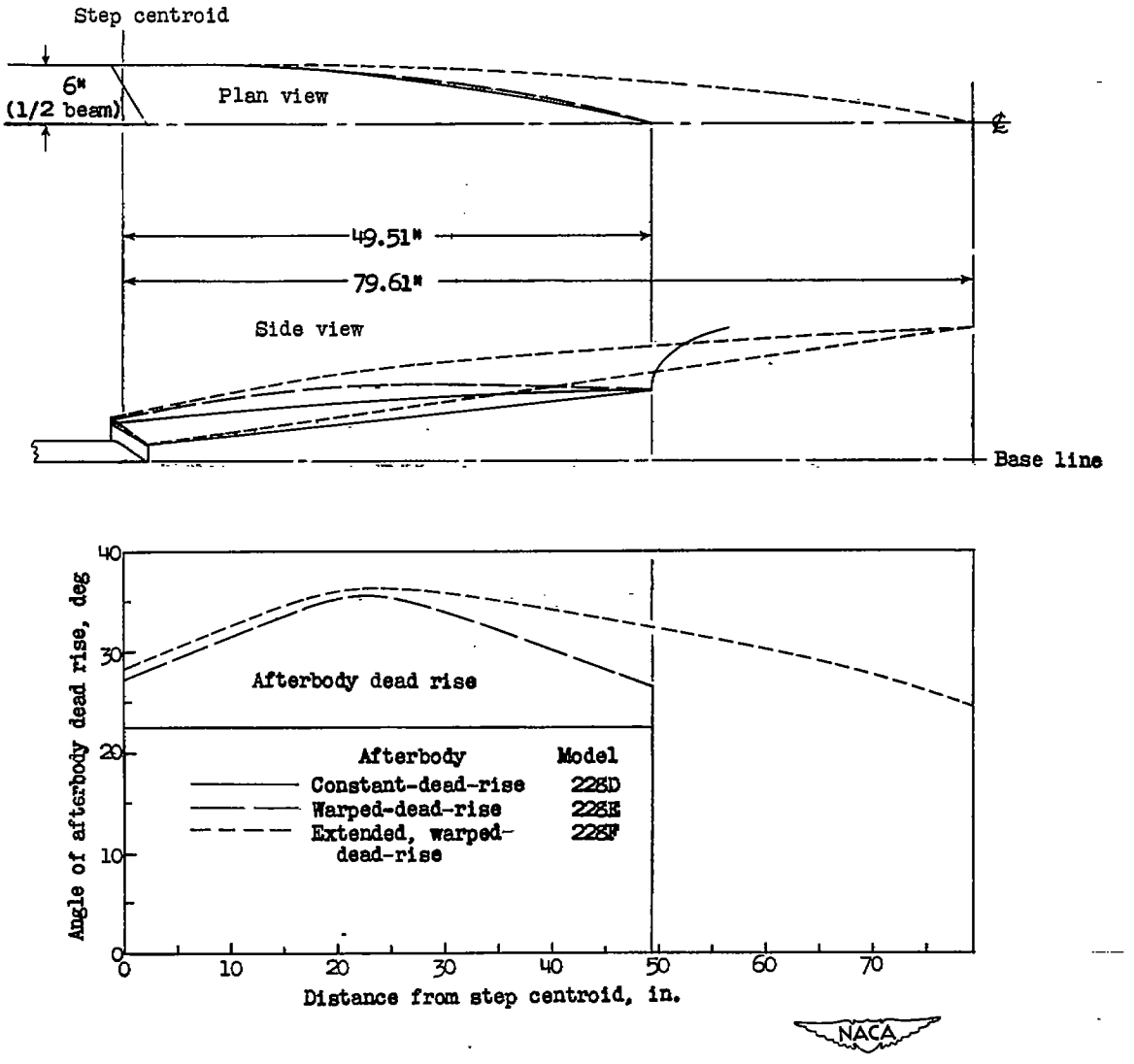

Figure 2.- Three afterbodies tested.

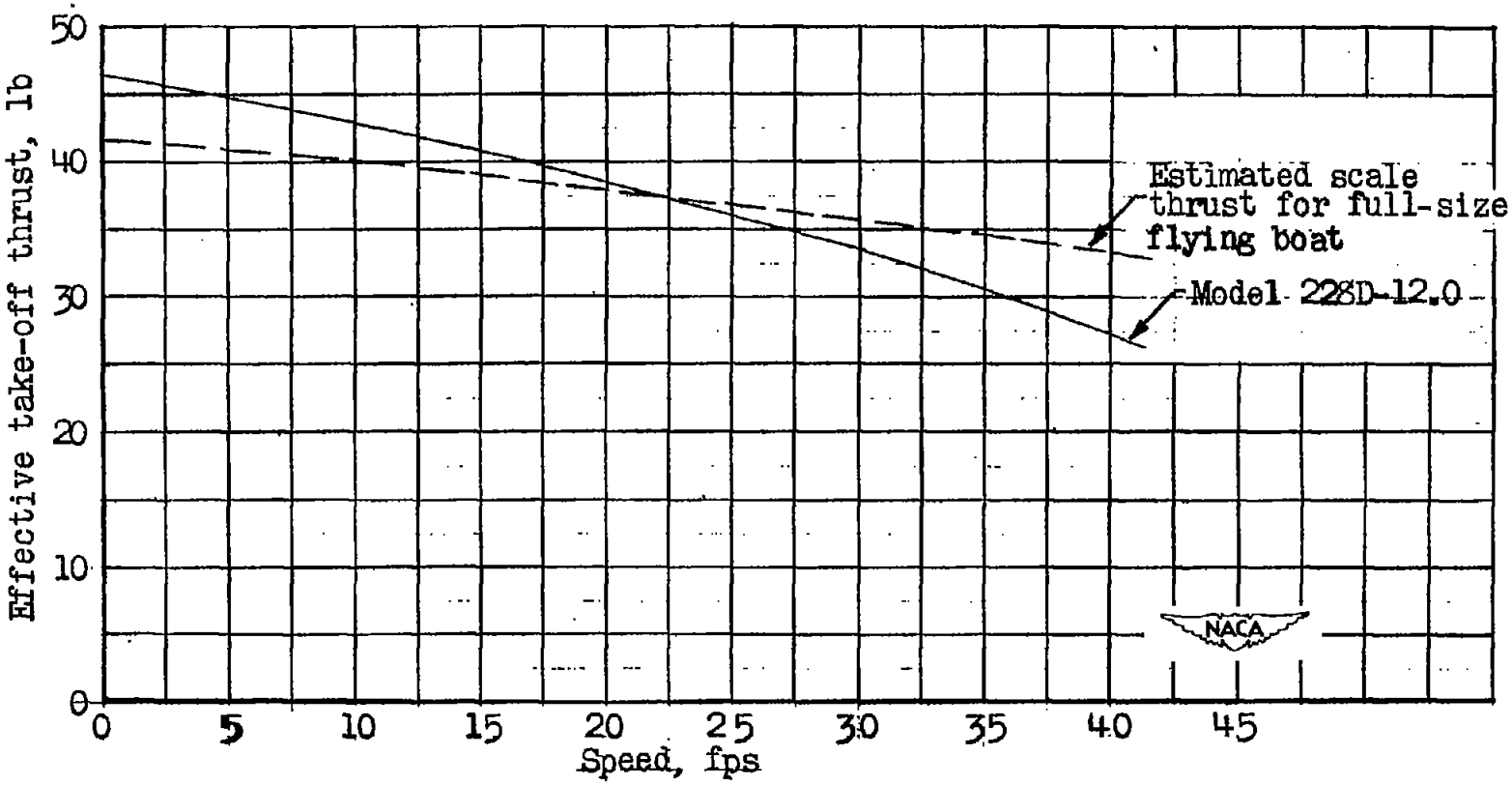

Figure 3.- Variation of effective take-off thrust with speed. Trim, 0°; flap deflection, 0°; elevator deflection, 0°.

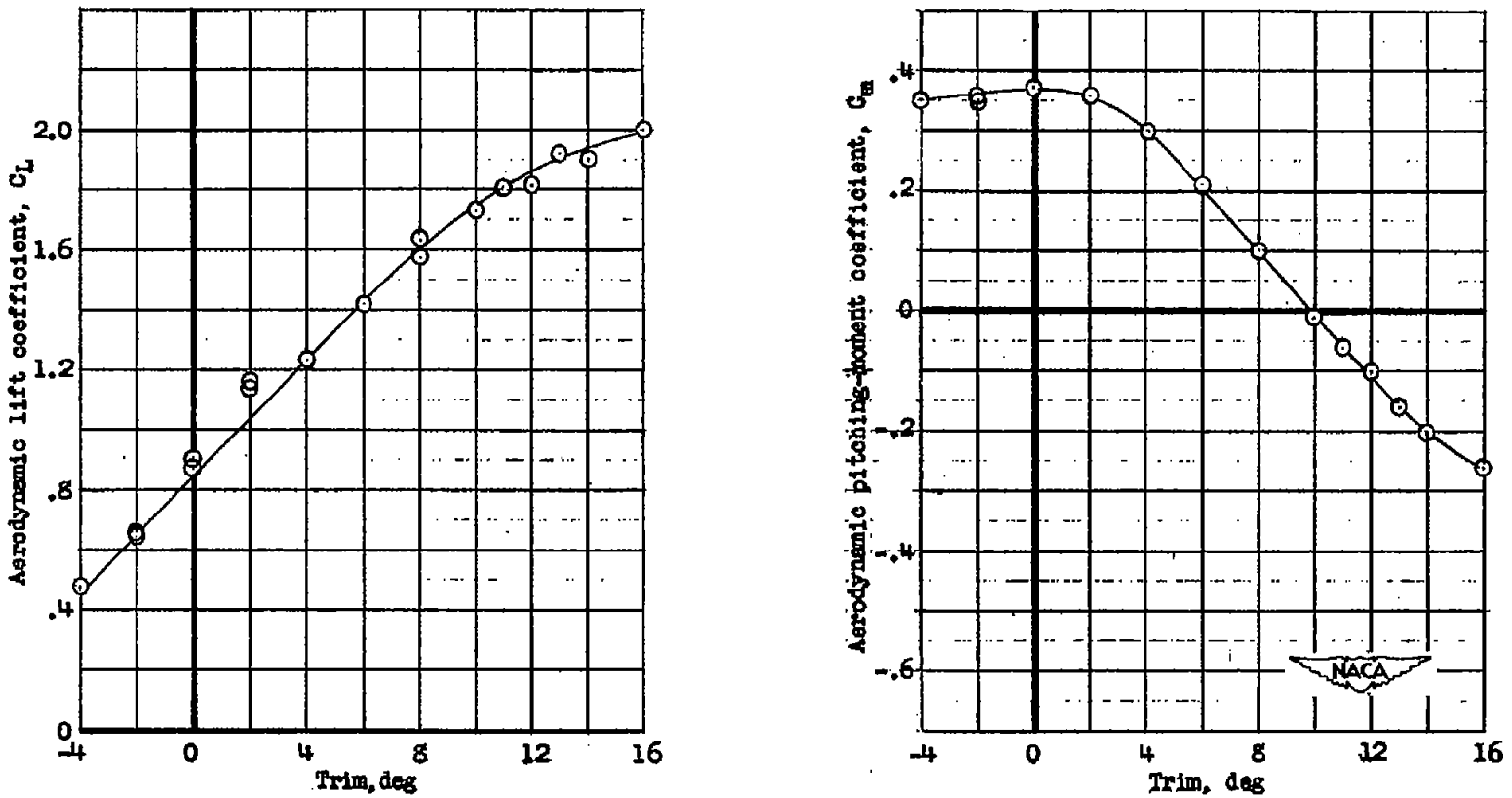

Figure 4.- Variation of aerodynamic lift and pitching-moment coefficients of model 22SD-12.0 with trim. Zero thrust; flap deflection, 50°; elevator deflection, -15°; center of moments, 25 percent M.A.C.

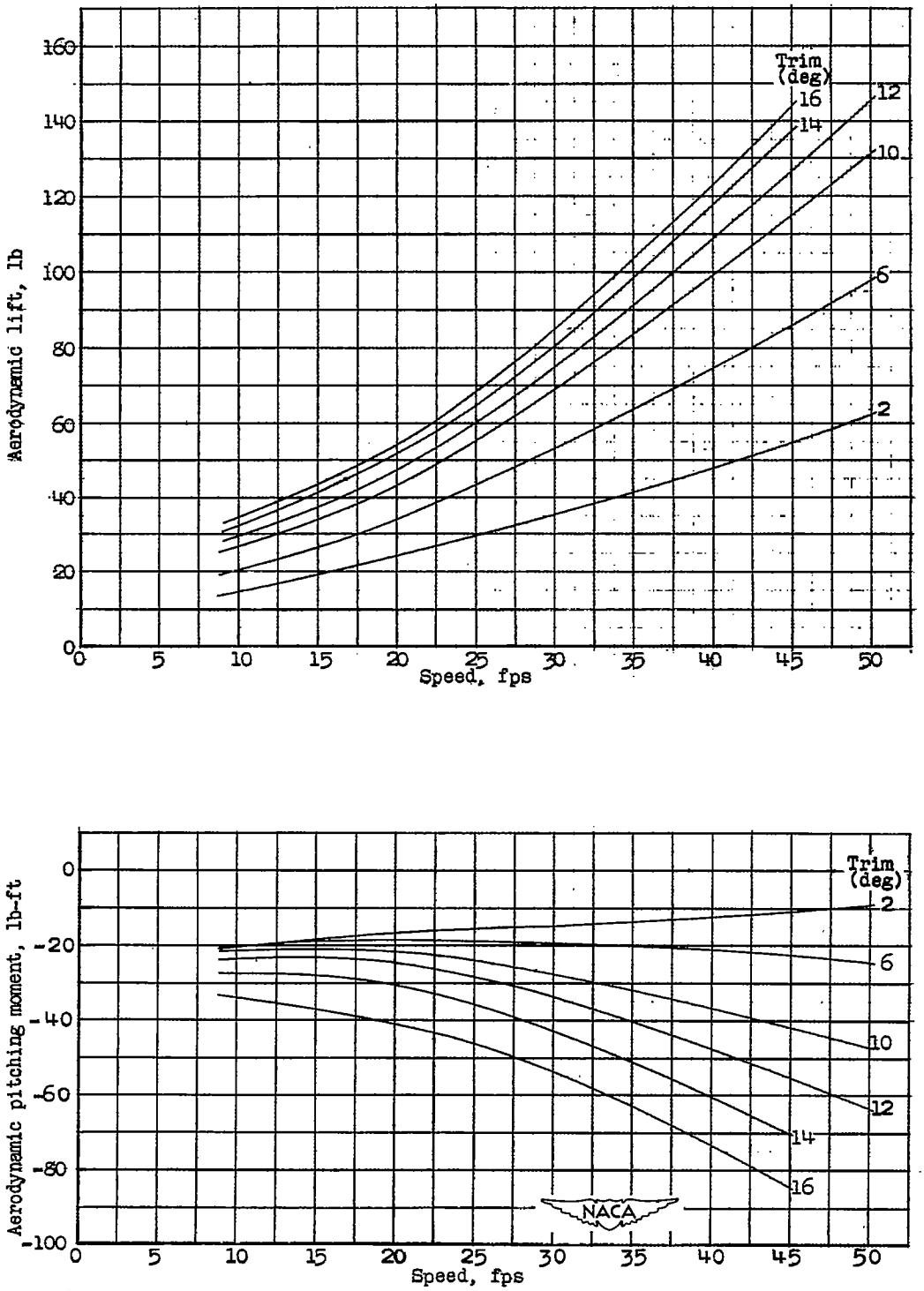

Figure 5.- Variation of aerodynamic lift and pitching moments of model 228D-12.0 with speed and trim. Take-off thrust; flap deflection, 20°; elevator deflection, 0°; center of moments, 25 percent M.A.C.

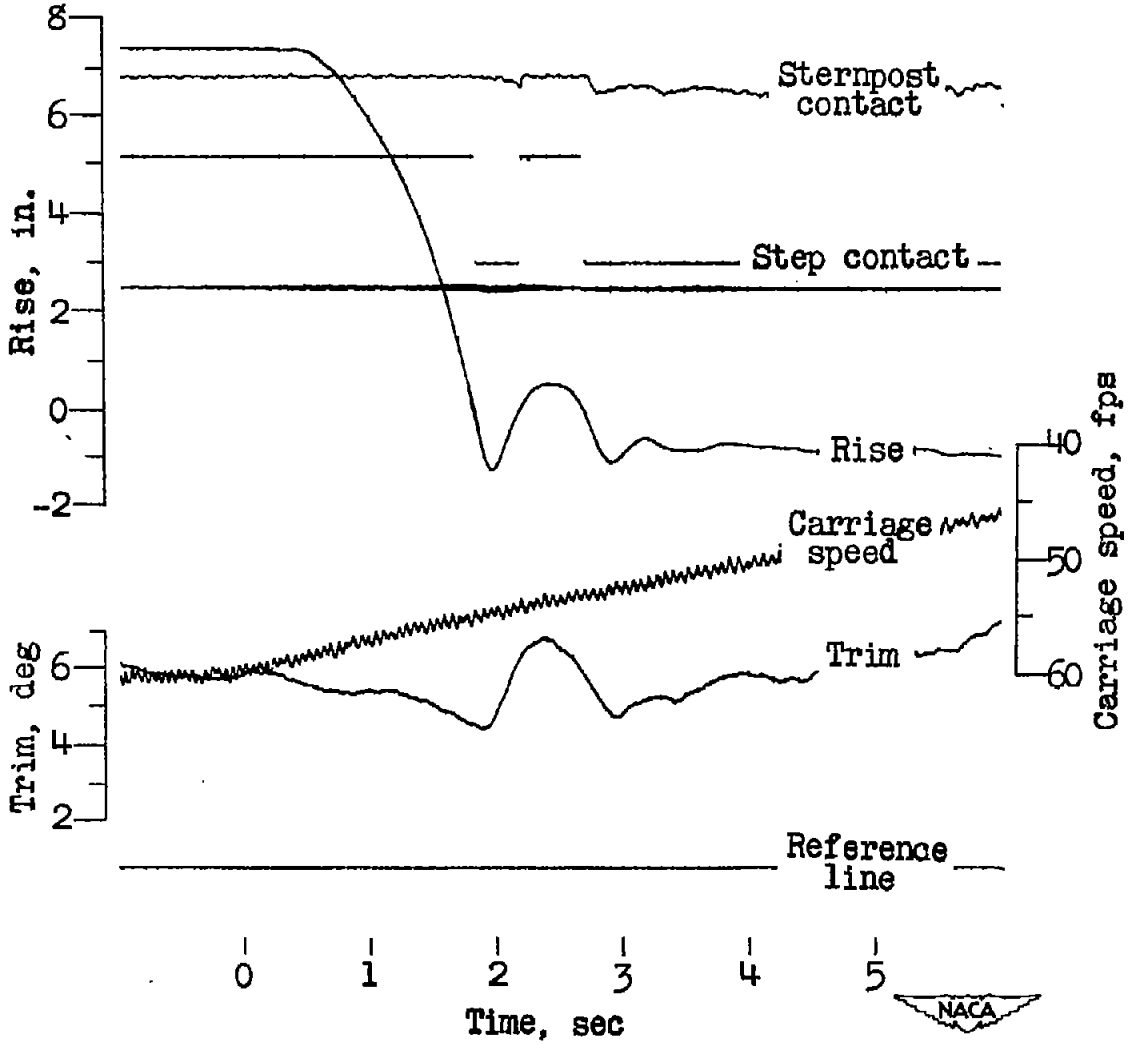

Figure 6.- Photograph of a typical oscillograph record taken during a landing.

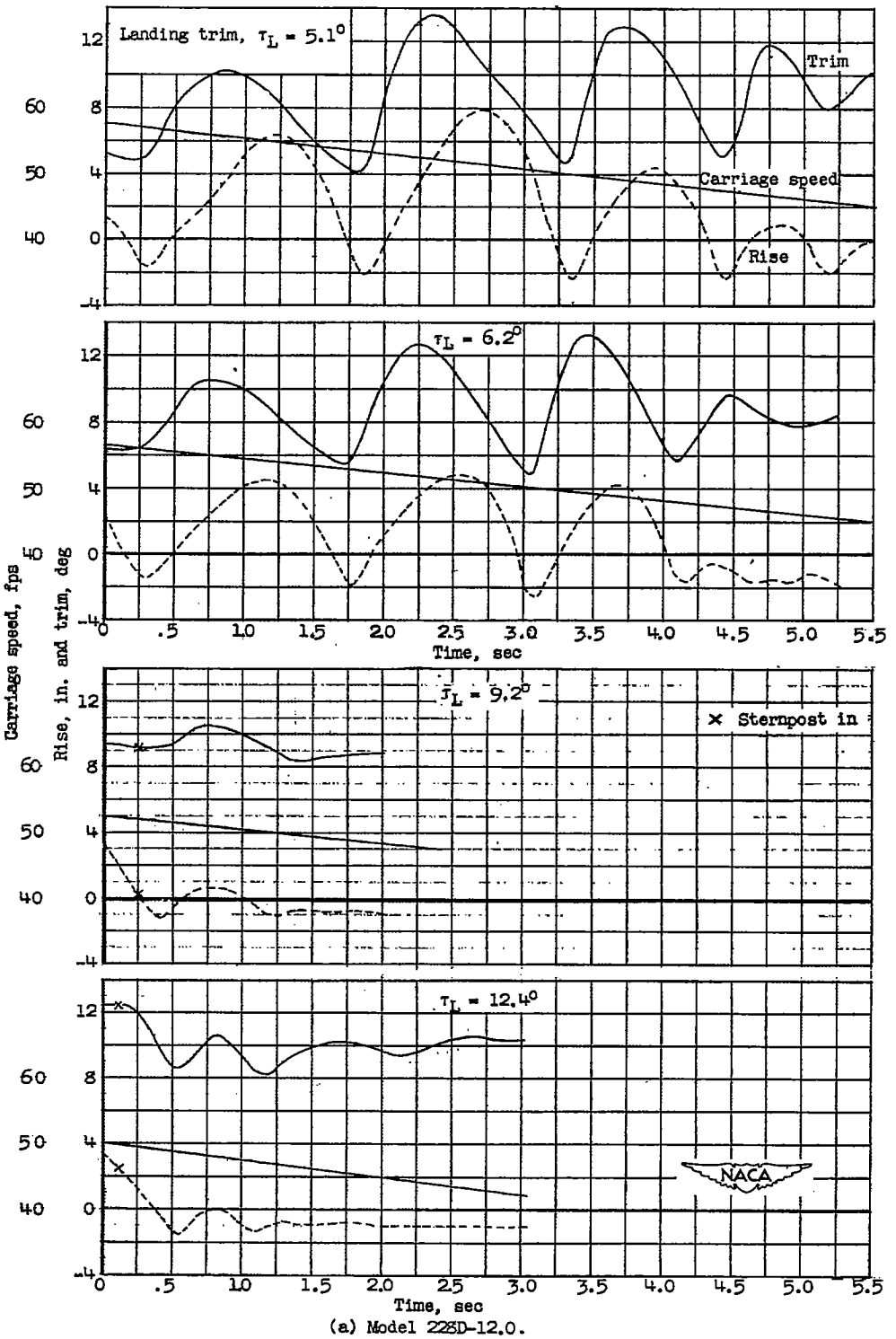

(a) Model 228D-12.0.

Figure 7.- Variation of rise, trim, and carriage speed during landing. Center of gravity, 34 percent M.A.C.

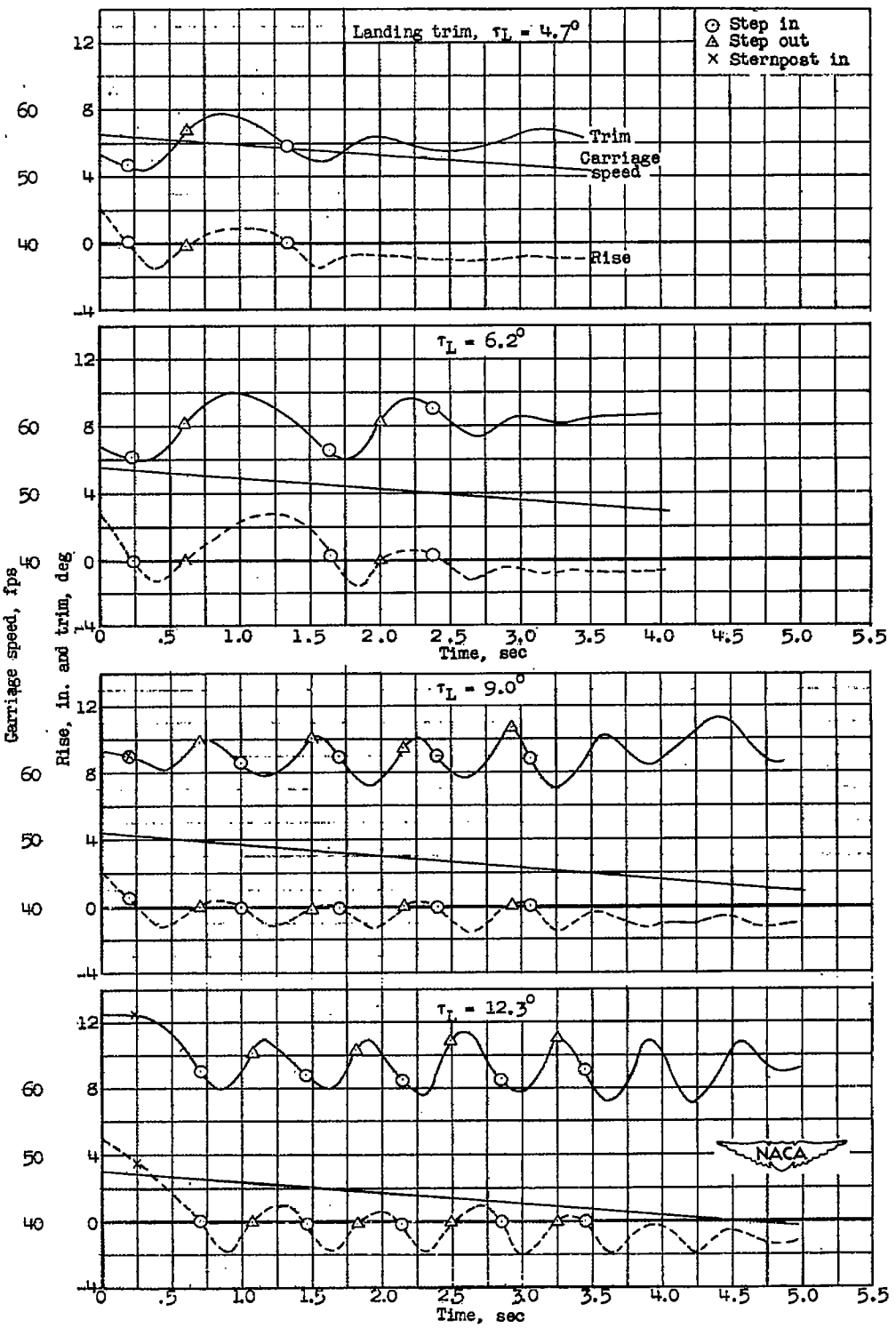

(b) Model 228E-10.8.

Figure 7.- Continued.

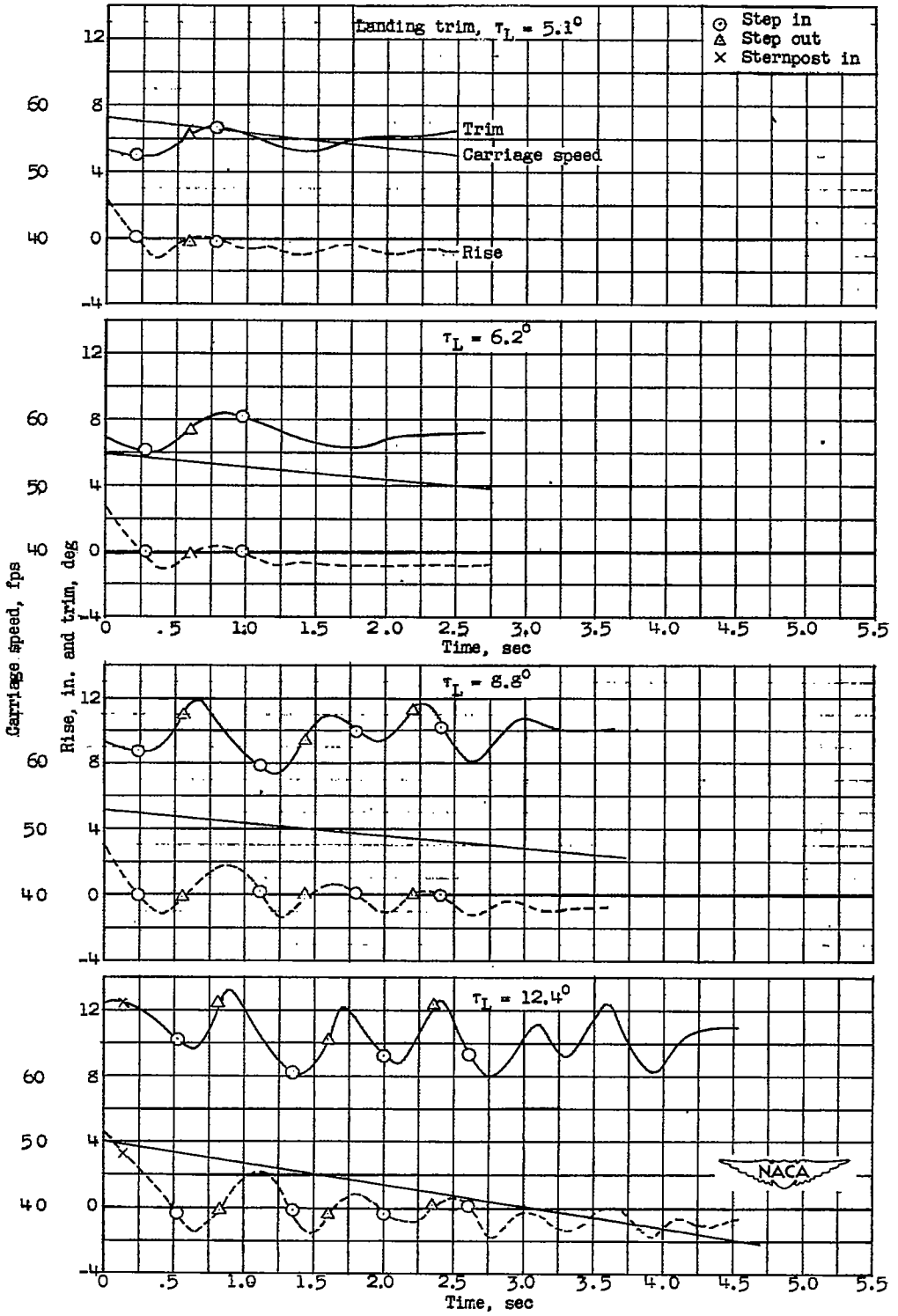

(c) Model 226F-18.4.

Figure 7.- Concluded.

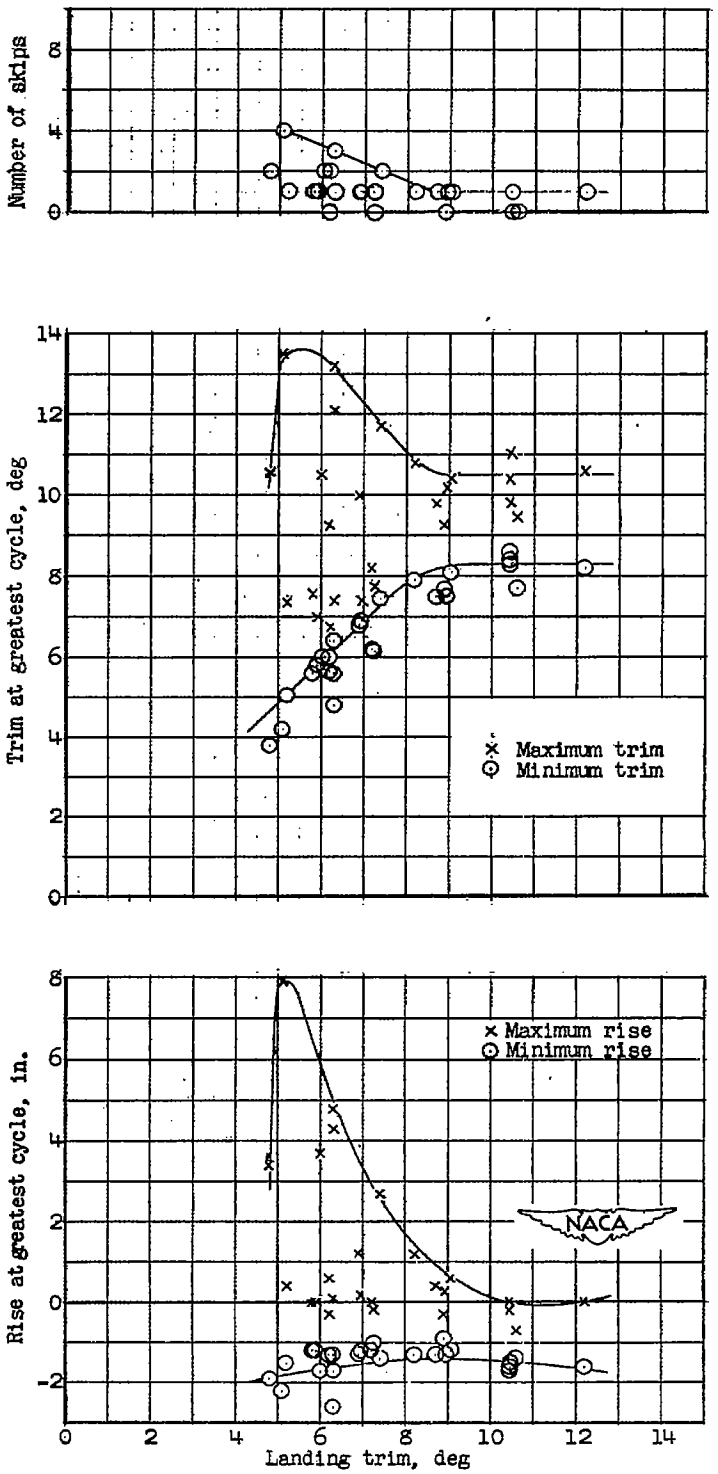

(a) Center of gravity, 34 percent M.A.C.

Figure 8.- Model 228D-12.0. Skipping characteristics during landing.

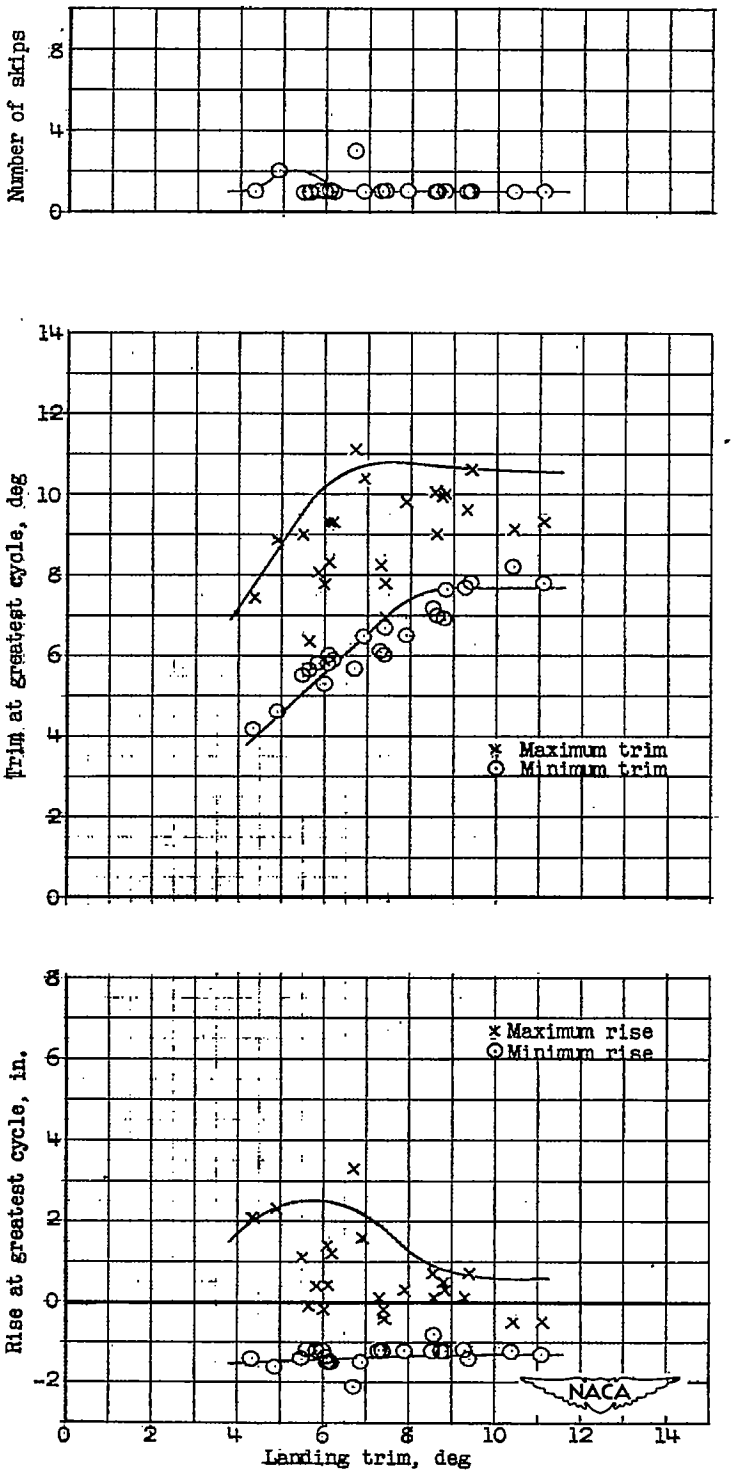

(b) Center of gravity, 26 percent M.A.C.

Figure 8.- Concluded.

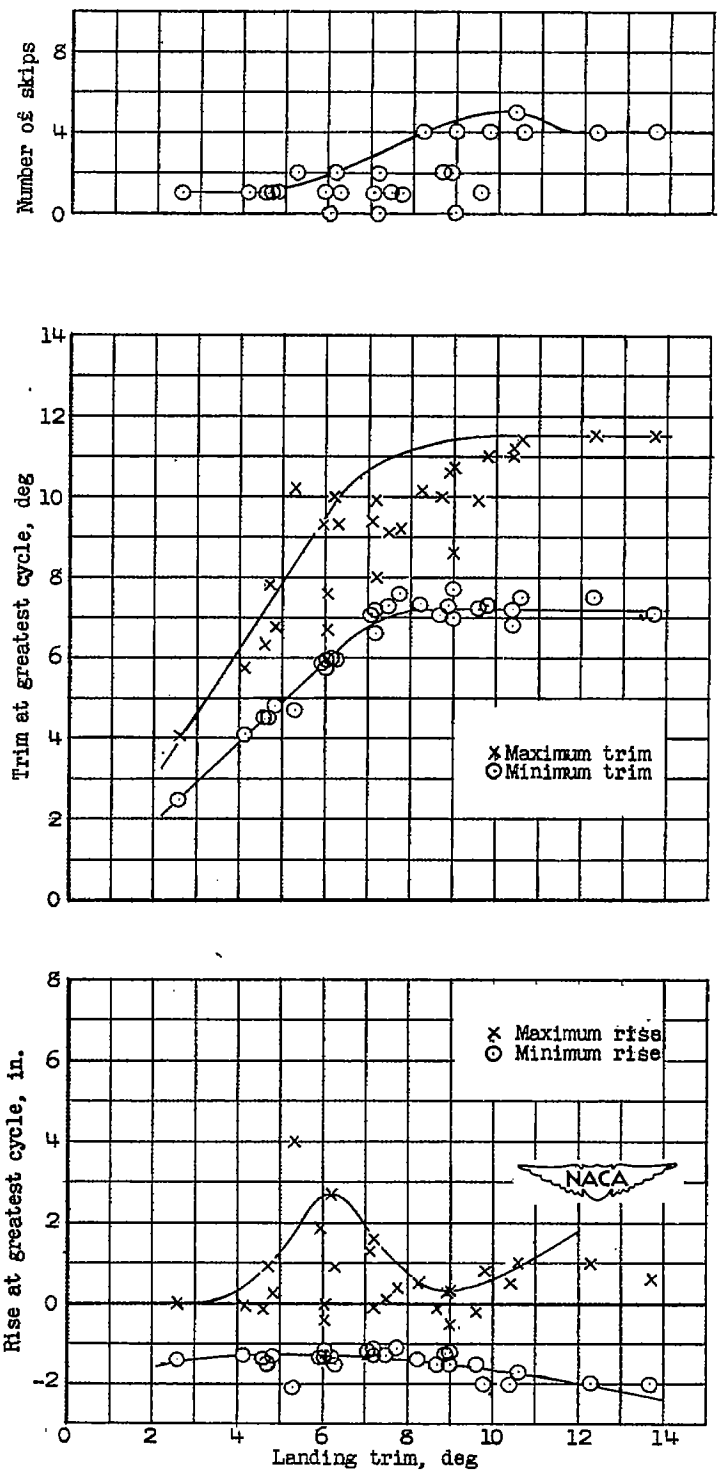

Figure 9.- Model 228E-10.8. Skipping characteristics during landing. Center of gravity, 34 percent M.A.C.

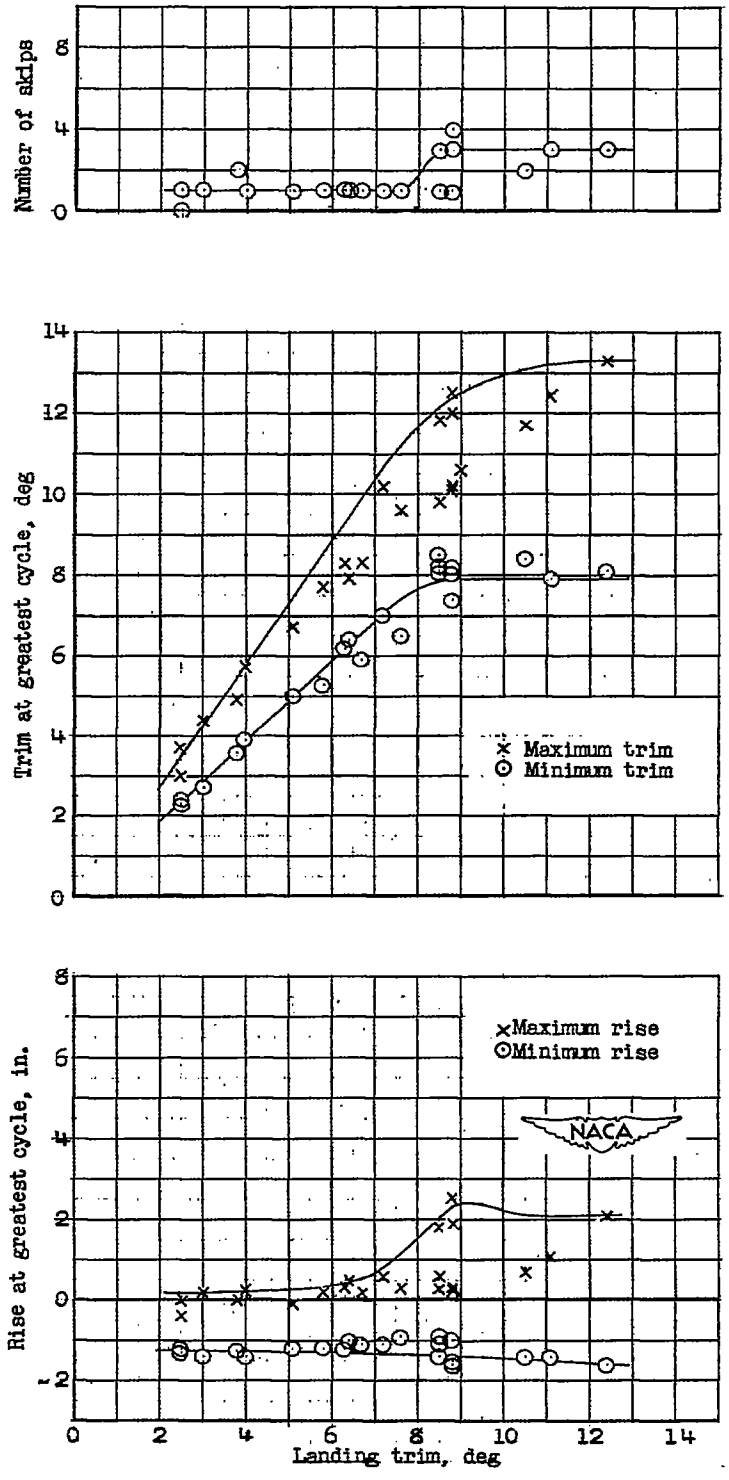

Figure 10.- Model 228F-16.4. Skipping characteristics during landing. Center of gravity, 34 percent M.A.C.

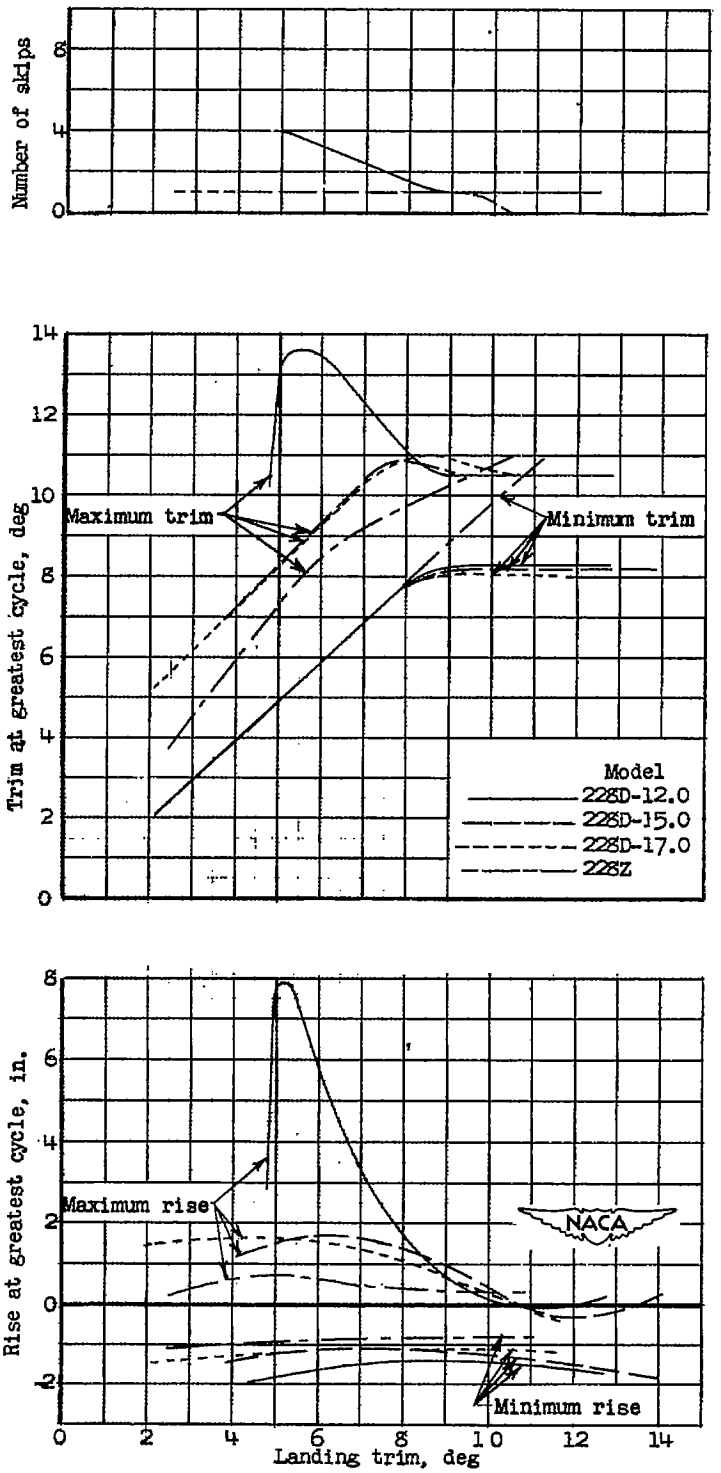

(a) Constant-dead-rise afterbody.

Figure 11.- Comparison of skipping characteristics during landing for different depths of step. Center of gravity, 34 percent M.A.C.

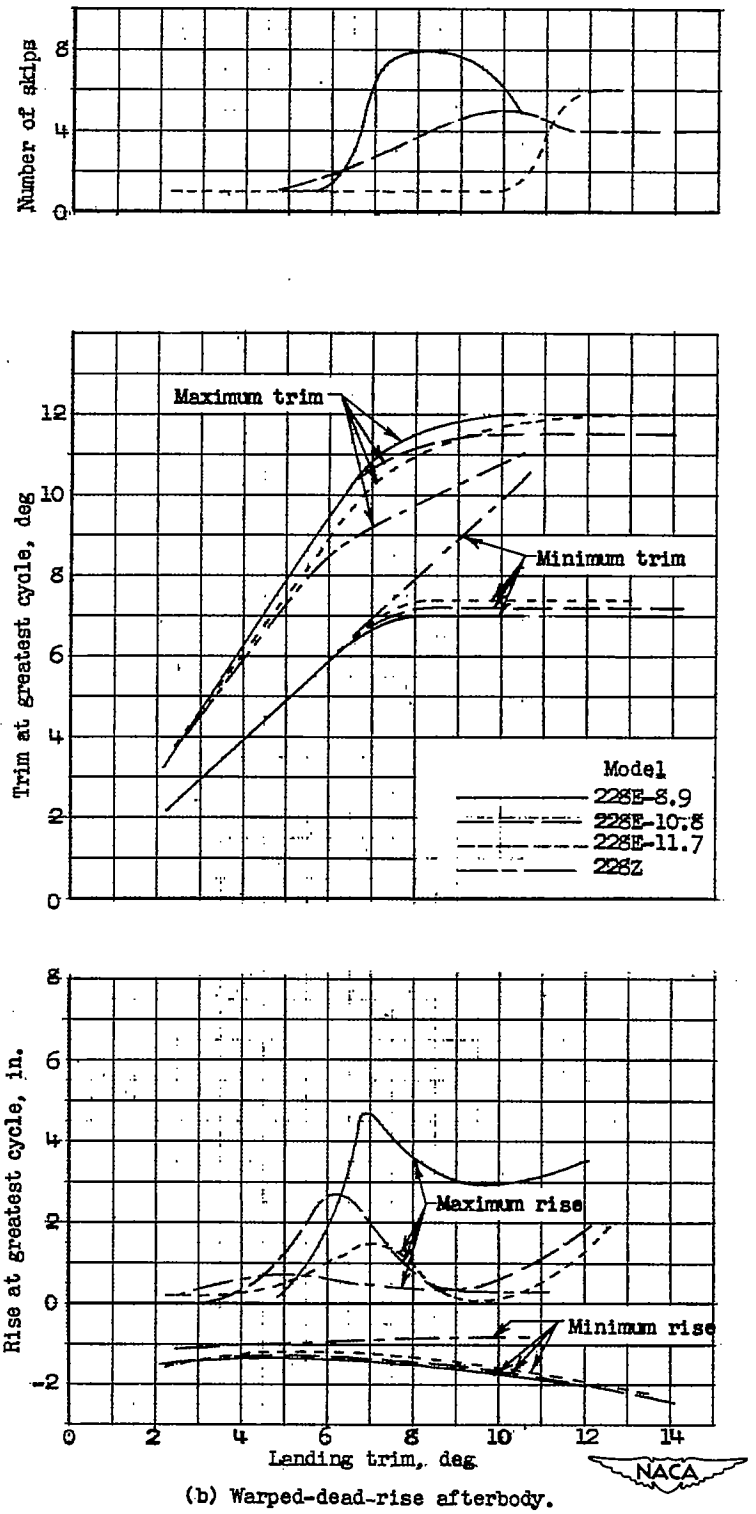

(b) Warped-dead-rise afterbody.

Figure 11.- Continued.

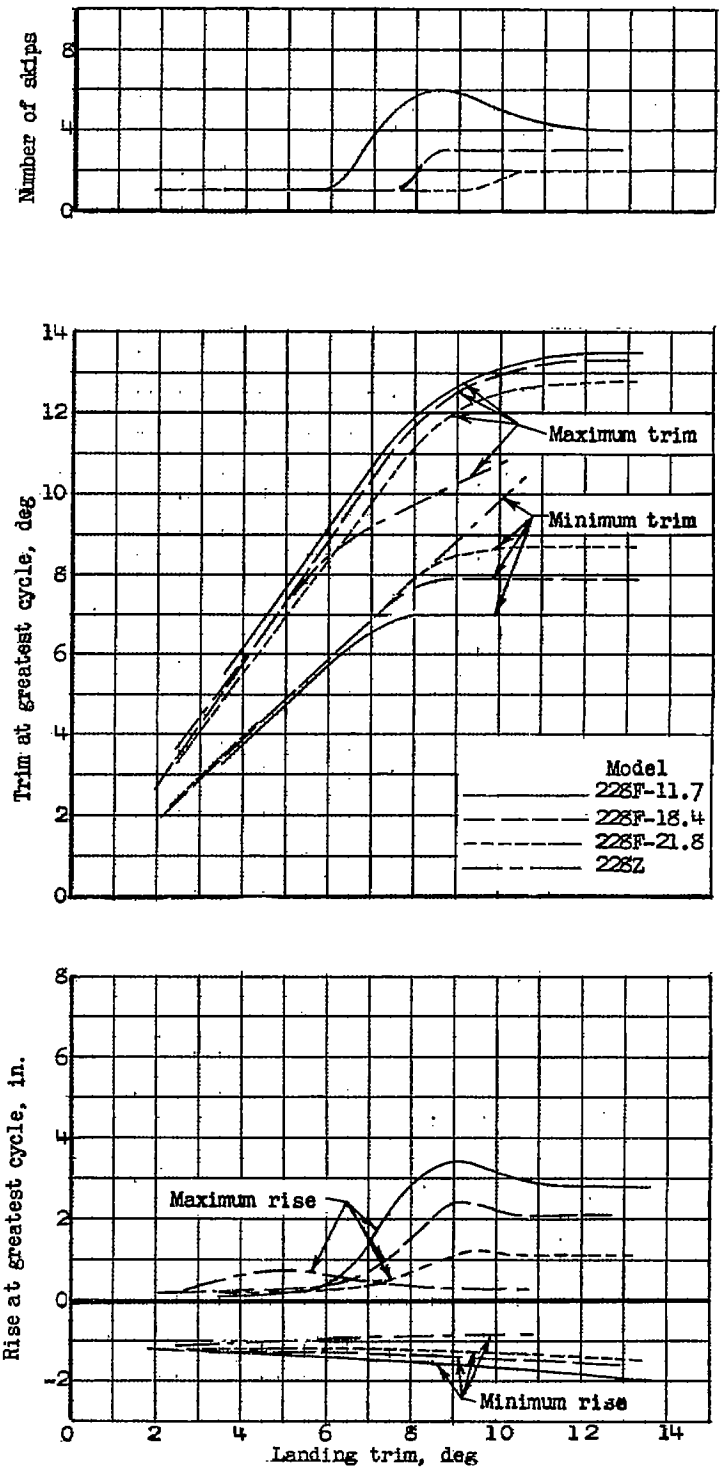

(c) Extended warped-dead-rise afterbody.

Figure 11.- Concluded.

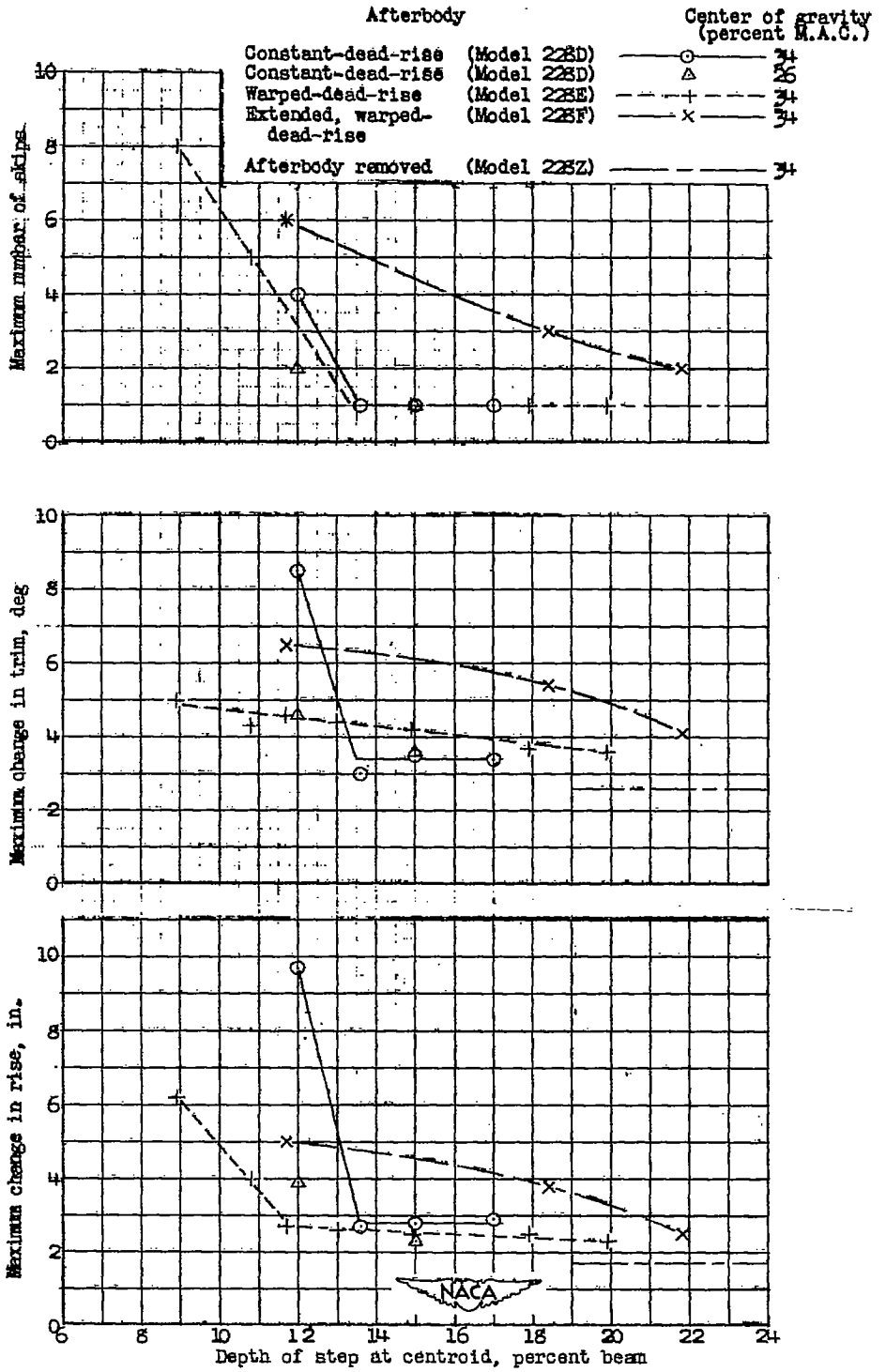

Figure 12.- Comparison of variations of maximum number of skips and maximum changes in trim and rise with depth of step for the three afterbodies.

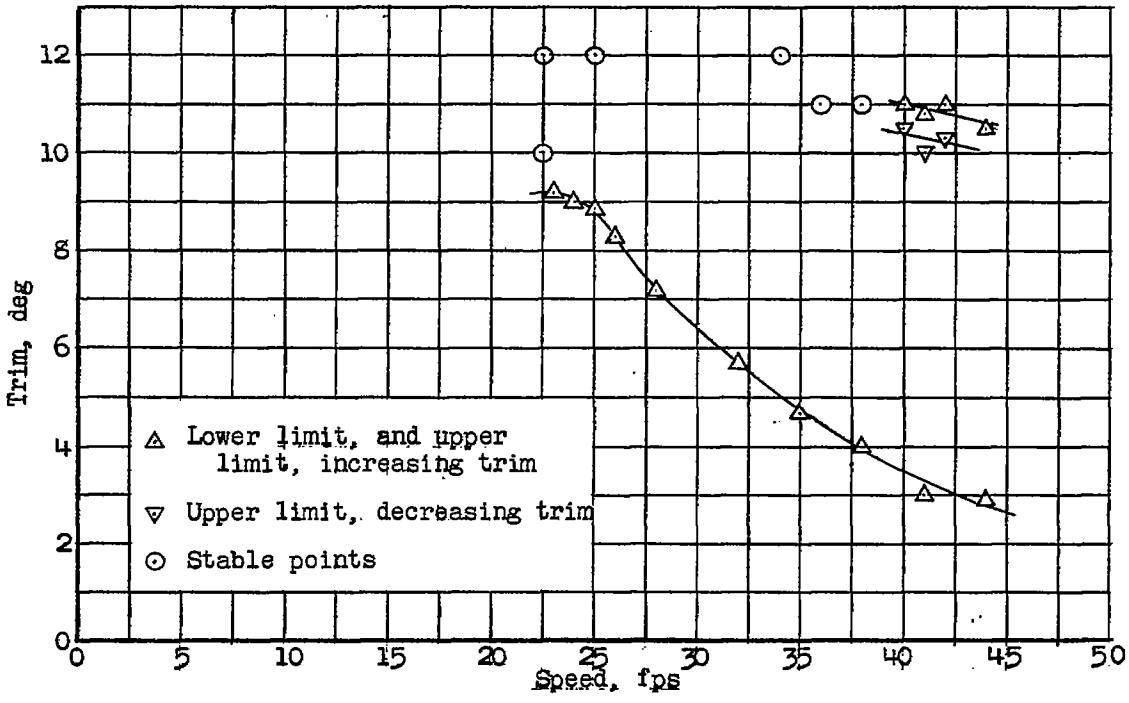

(a) Model 228D-15.0.

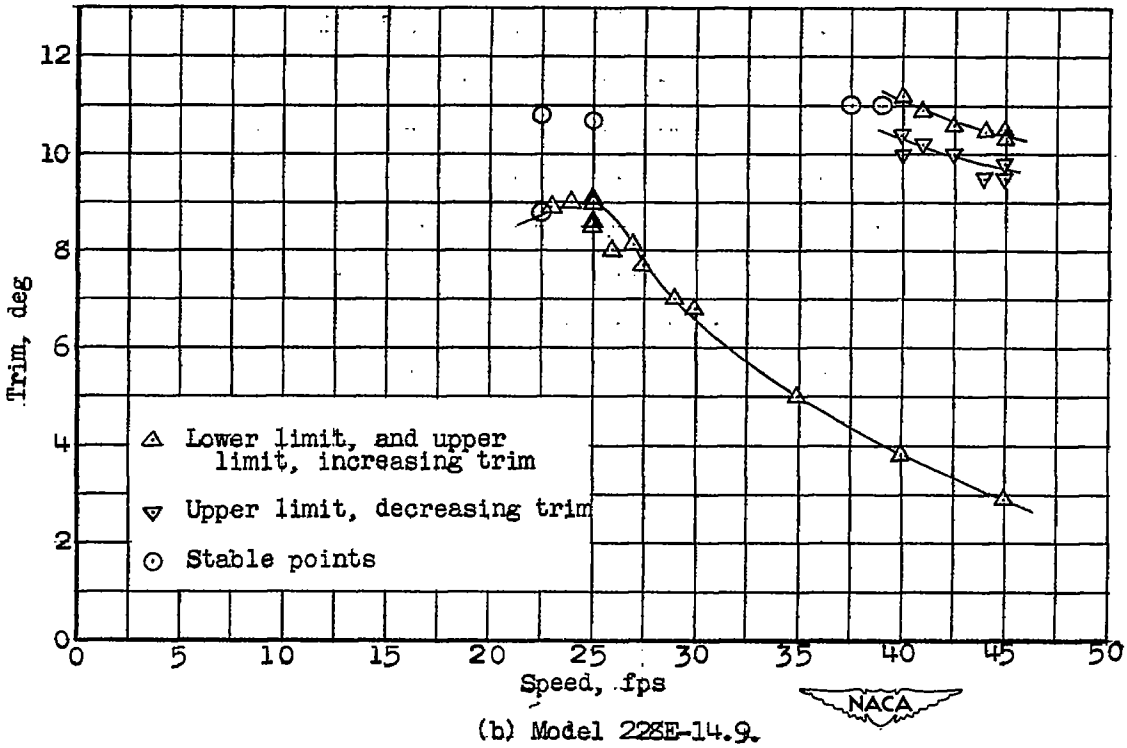

(b) Model 228E-14.9.

Figure 13.- Trim limits of stability for the take-off condition.

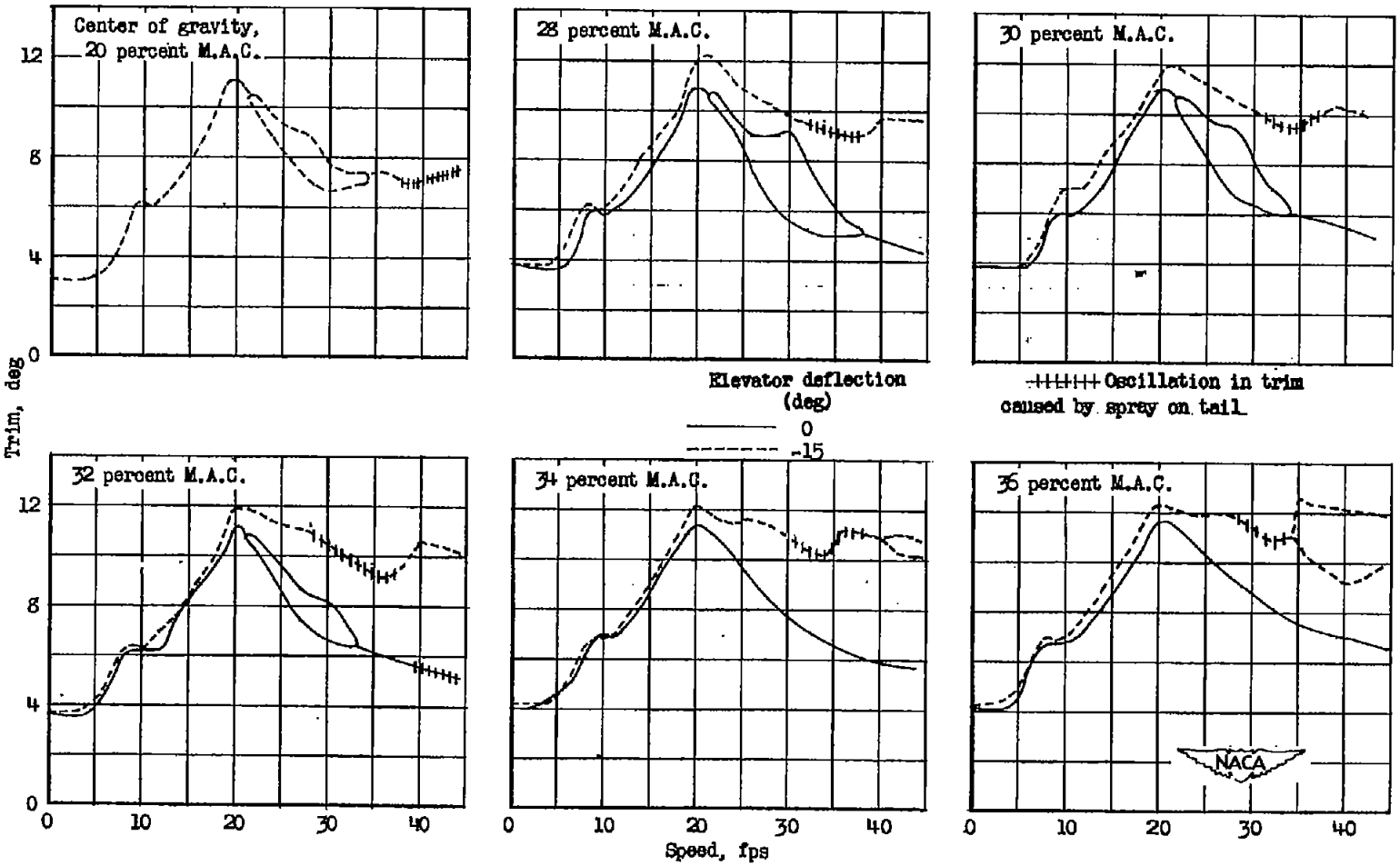

(a) Model 228D-15.0.

Figure 14.- Variation of trim with speed during take-off.

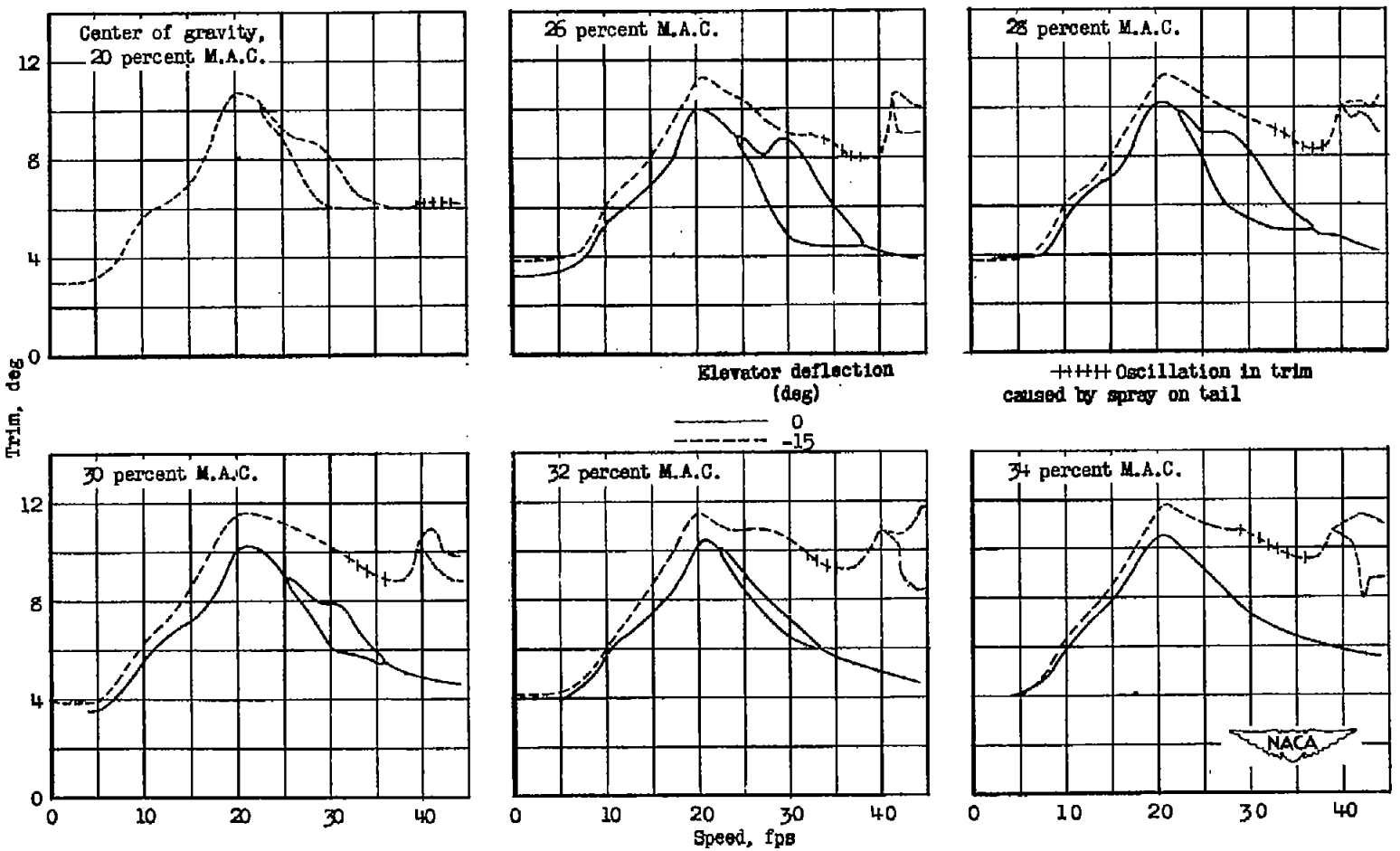

(b) Model 228E-14.9.

Figure 14.- Continued.

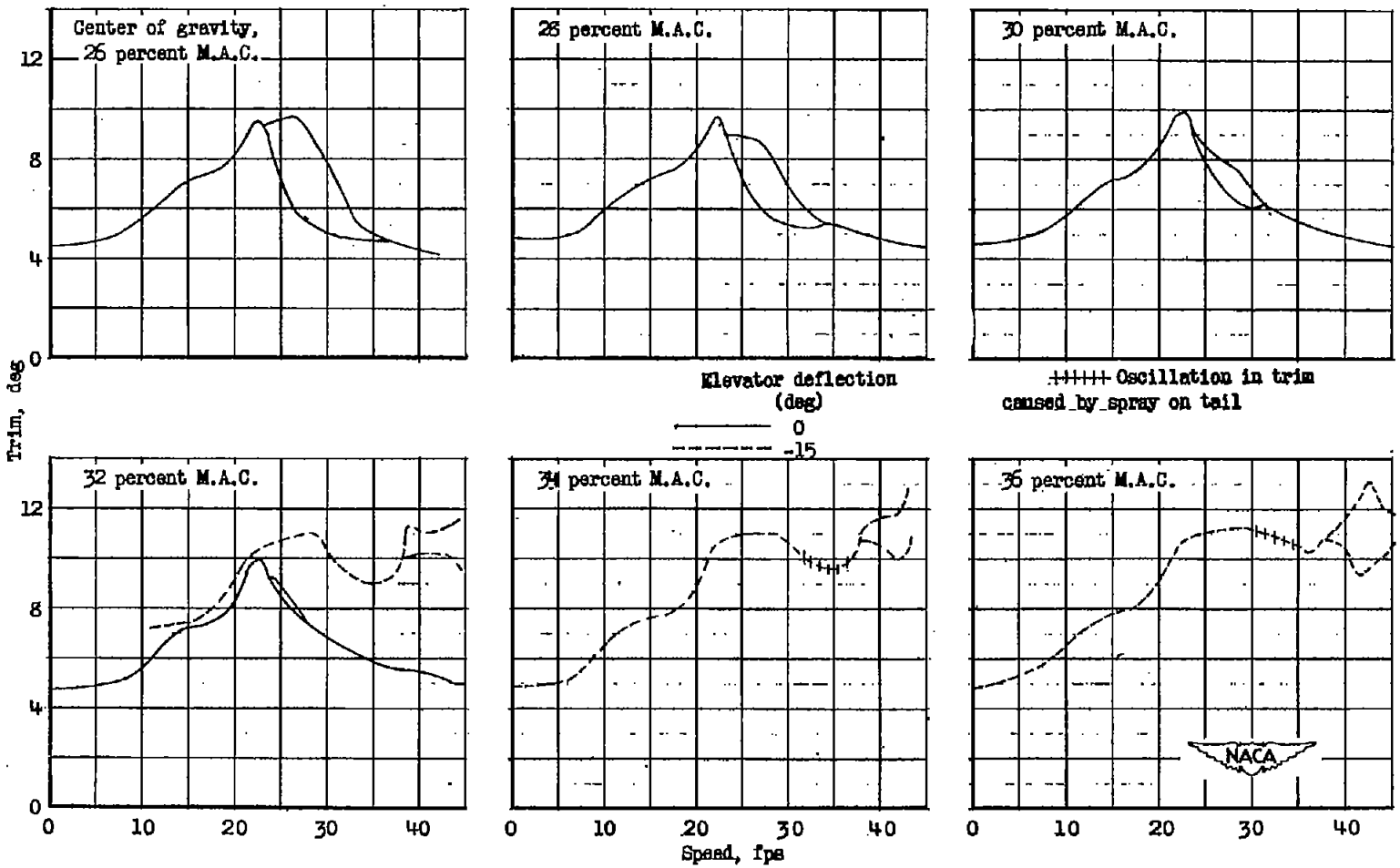

(c) Model 22EF-21.8.

Figure 14.- Concluded.

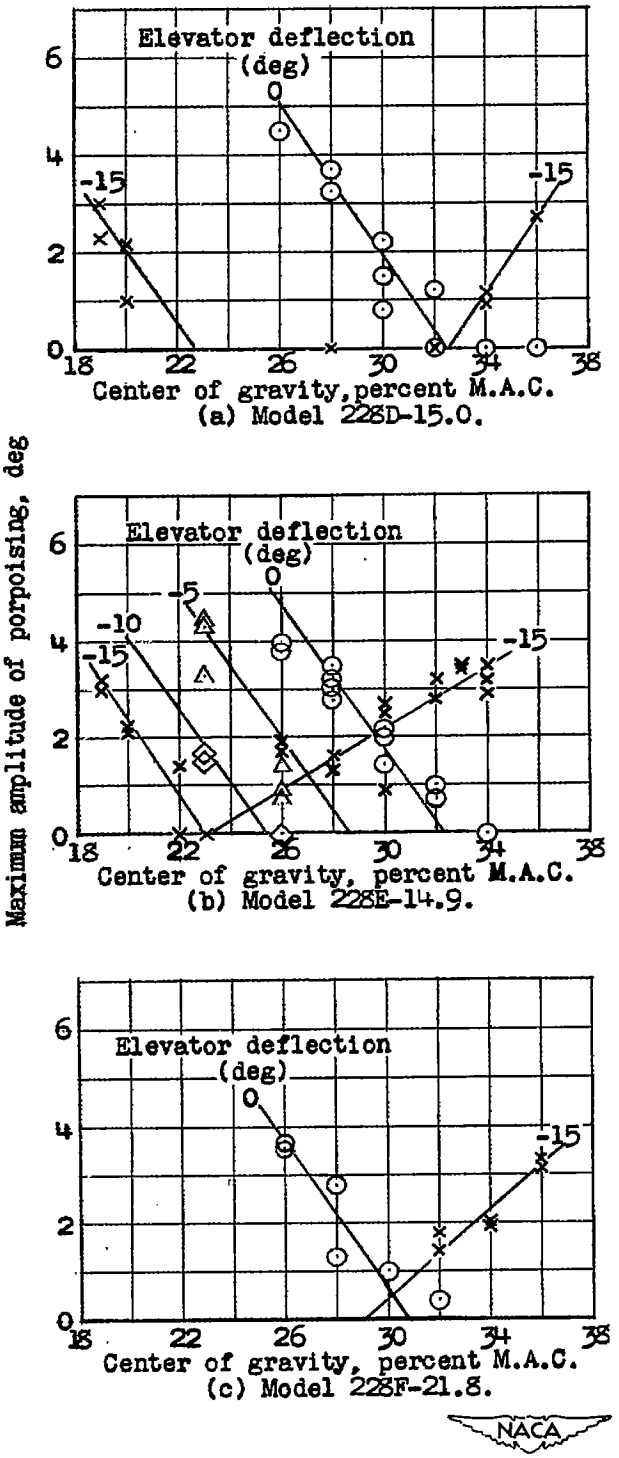

Figure 15.- Variation of maximum amplitude of porpoising during take-off with position of the center of gravity.

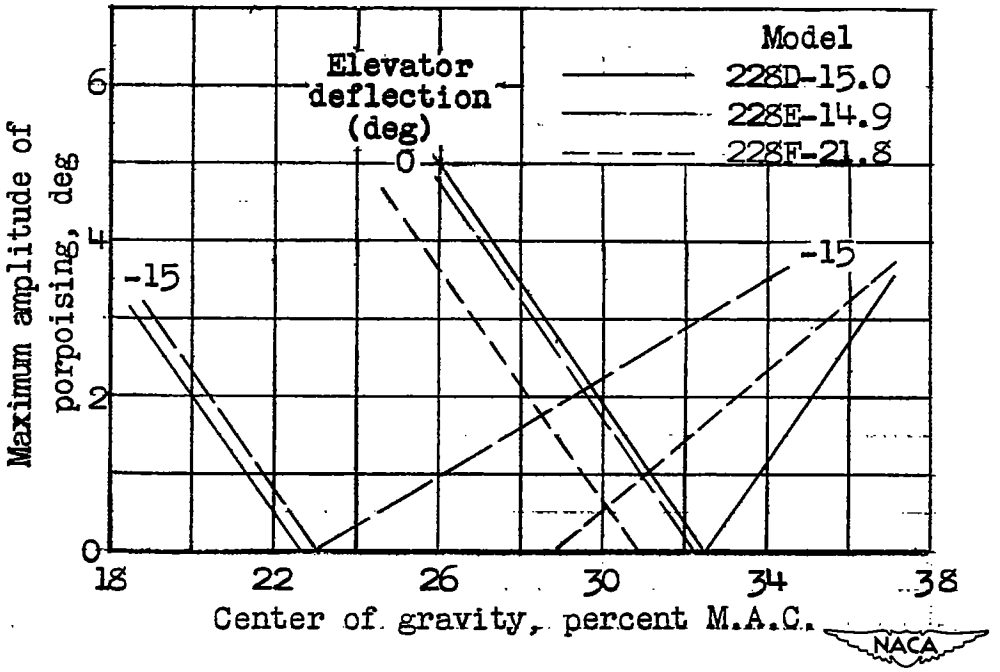

Figure 16.- Comparison of variations of maximum amplitude of porpoising during take-off with position of the center of gravity.

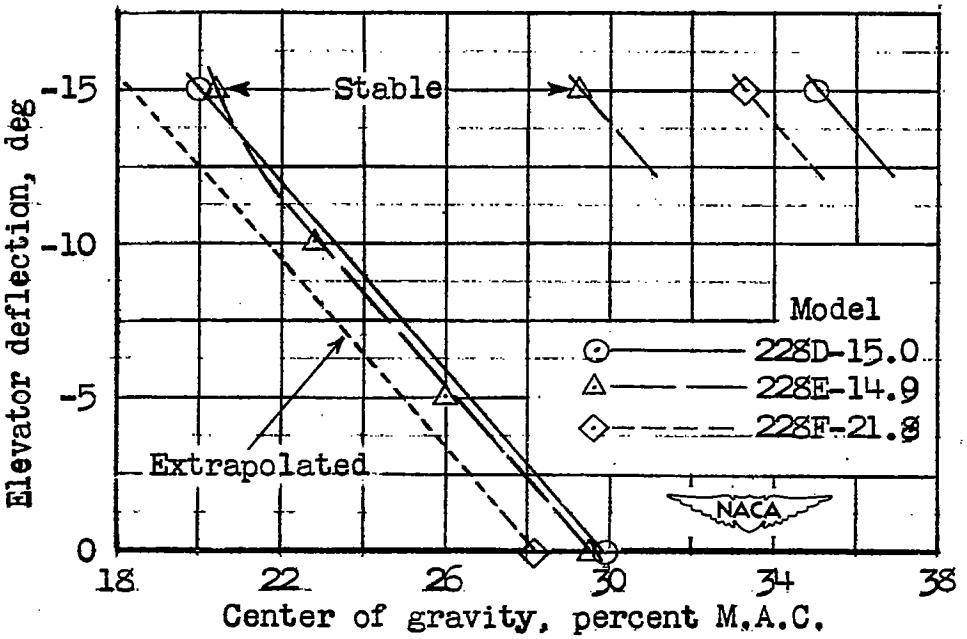

Figure 17.- Comparison of ranges of position of the center of gravity for satisfactory take-off (2° maximum amplitude of porpoising).

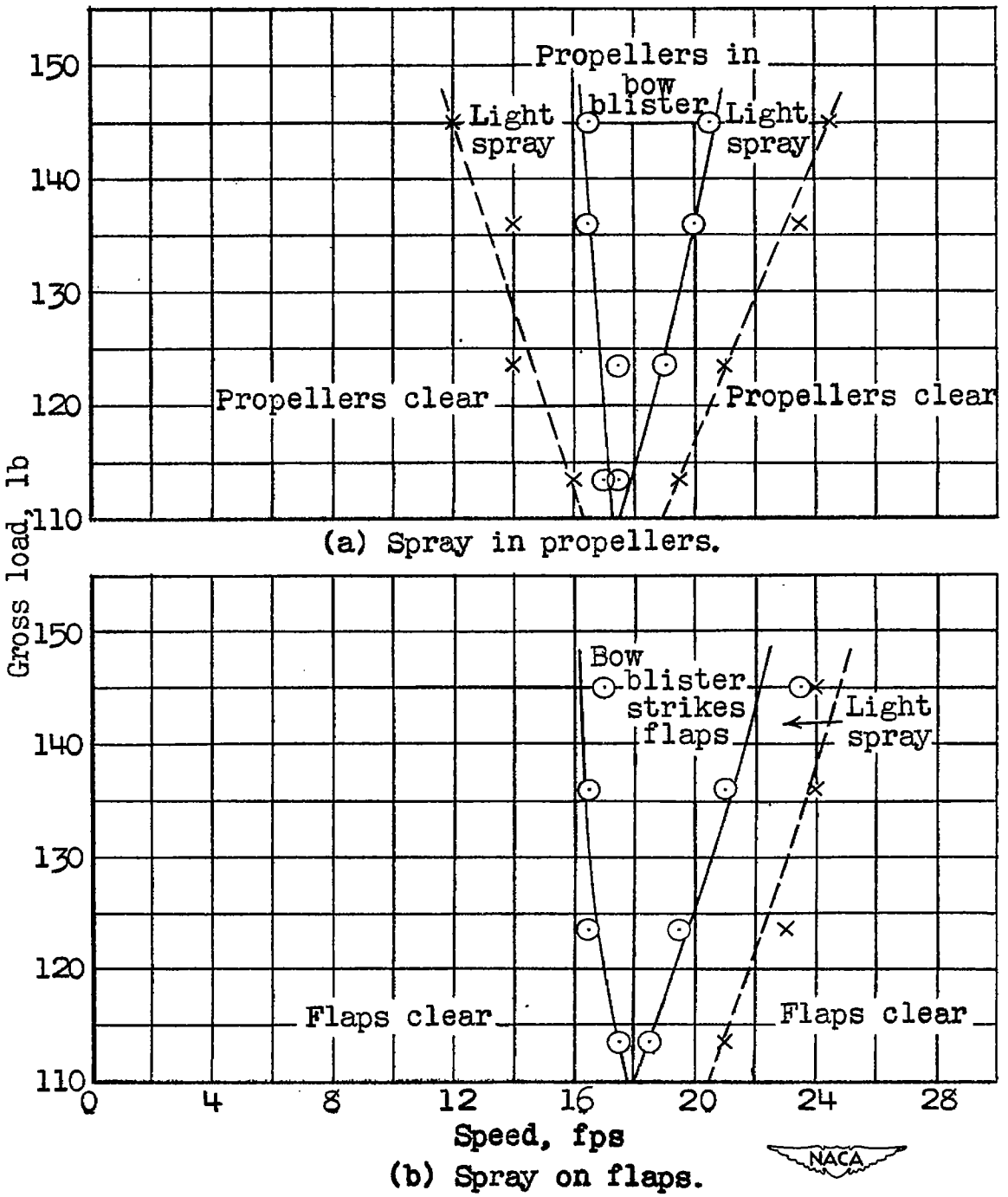

Figure 18.- Model 228D-15.0. Speed range in which spray strikes the propellers and flaps.